BY ORDER OF THE COMMANDER

SMC Standard SMC-S-015
19 March 2010

Supersedes:
SMC-S-015 (2008)

Air Force Space Command

SPACE AND MISSILE SYSTEMS CENTER STANDARD

END-OF-LIFE DISPOSAL OF SATELLITES IN GEOSYNCHRONOUS ALTITUDE

APPROVED FOR PUBLIC RELEASE; DISTRIBUTION IS UNLIMITED

FOREWORD

1. This standard defines the Government's requirements and expectations for contractor performance in defense system acquisitions and technology developments.

2. This revised SMC standard comprises the text of The Aerospace Corporation report number TOR-2006(8583)-4474, Rev A (18 August 2009), entitled *Requirements for End-of-Life Disposal of Satellites Operating at Geosynchronous Altitude: Revision A* and contains the following major changes:

- Moved reference documents to Appendix A
- Added symbol/acronym for solar longitude
- Changed reliability for disposal from 'exceeds 0.95' to 'exceeds 0.90'
- Changed disposal planning requirement for limiting eccentricity from '0.005' to '0.003'
- Added description of required force models and precision of long-term orbit propagation to Section 6.4
- Footnote added after Table A.1 explaining additional burns after minimum perigee increase is satisfied
- Paragraph added after Table A.1 and A.2 to discuss ground-station-viewing constant.

3. Beneficial comments (recommendations, changes, additions, deletions, etc.) and any pertinent data that may be of use in improving this standard should be forwarded to the following addressee using the Standardization Document Improvement Proposal appearing at the end of this document or by letter:

Division Chief, SMC/EAE
SPACE AND MISSILE SYSTEMS CENTER
Air Force Space Command
483 N. Aviation Blvd.
El Segundo, CA 90245

4. This standard has been approved for use on all Space and Missile Systems Center/Air Force Program Executive Office - Space development, acquisition, and sustainment contracts.

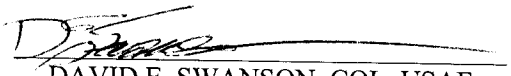

DAVID E. SWANSON, COL, USAF
SMC Chief Engineer

Errata

Page 13, Section 6.5: "Equation 7.2" should read, "Equation 6.2".

Page 14, Section 6.5: "… using steps outlined in paragraphs 7.3 and 7.4"
should read,
"… using steps outlined in paragraphs 6.3 and 6.4".

Contents

Figures

Tables

1. Scope

End-of-life disposal of an Earth-orbiting satellite means 1) removing the satellite from the region of space where other satellites are operating so as not to interfere with these other users of space in the future, and 2) assuring that the disposed object is left in an inert state and not capable of an internally generated explosive event that could release debris and threaten operating satellites. For satellites operating in the geosynchronous belt, the most effective means of disposal is to reorbit the satellite to a super-synchronous orbit, above the region of operating spacecraft and the maneuver corridor used for relocating operating satellites to new longitudinal slots, and then to discharge batteries, vent propellants, and take other actions to eliminate the possibility of a debris-producing event.

This report specifies requirements for 1) planning for disposal of satellites operating at geosynchronous altitude to ensure that final disposal is sufficiently characterized that adequate propellant will be reserved for the maneuver, 2) selecting final disposal orbits where the satellite will not reenter the operational region in the foreseeable future, 3) executing the disposal maneuver successfully, and 4) depleting all energy sources onboard the vehicle prior to end-of-life to minimize the possibility of a debris-producing event. Techniques for planning and executing space hardware disposal are provided that reflect current internationally accepted guidelines and consider current operational best practices. This revision incorporates the results of recent technical studies by the Inter-Agency Space Debris Coordination Committee on limiting the initial eccentricity of the disposal orbit to ensure that the disposed satellite does not reenter the region of operating and maneuvering satellites for at least 100 years.

2. Application

These requirements shall be applied to the end-of-mission disposal of satellites operating at geosynchronous altitude.

3. Terms and Definitions

3.1 End of Life

The point where a satellite is permanently "turned off" or where control of the satellite from the ground is no longer possible.

3.2 End of Mission

End of mission refers to the point in a satellite's lifetime when 1) it is unable to perform the primary missions and no longer requires operation at the nominal operational altitude, or 2) the fuel remaining, attitude control, or other function critical to performing a successful disposal maneuver reaches a level or capability where further delay would make completion of the disposal maneuver unlikely.

3.3 Geosynchronous Region

The geosynchronous region may be defined as a circular ring around the Earth in the Earth's equatorial plane. The mean angular rate of a space object moving along the ring is equal or very close to the Earth's rotation rate, meaning that the satellite appears to be positioned over a fixed ground location.

Without so-called "north-south" stationkeeping, the inclination of a GEO satellite will gradually cycle between zero degrees (equatorial orbit) to a maximum of approximately 14.6 degrees and back again. In addition to maintaining the accuracy of its inclination, a GEO satellite must execute station-keeping maneuvers to maintain longitudinal accuracy in order to prevent a naturally occurring drift to the east or to the west caused by asymmetries in the Earth's gravitational field, unless the spacecraft is located at one of the two "gravity wells" on the geostationary arc.

Figure 4.1 shows a three-dimensional view of the geosynchronous ring with a cross section defining the approximate size of the ring. Figure 4.2 gives the dimensions of three regions of the cross section. The cross section is defined by two axes: the latitude axis and radial axis. This plane of the cross section is perpendicular to the Earth's equatorial plane.

The three concentric boxes shown in Fig. 4.2 give the approximate boundaries for three types of orbits. The smallest box represents the region where a geostationary satellite will be confined under stationkeeping, and the next larger box approximates the region for a geosynchronous satellite whose inclination is not controlled but remains under a desired value of 3 to 5 deg. The largest box represents the inclination excursion region for a non-operational GEO satellite and the ±200-km protected region. For most communication satellites, the longitude stationkeeping limit is ±0.1 deg.

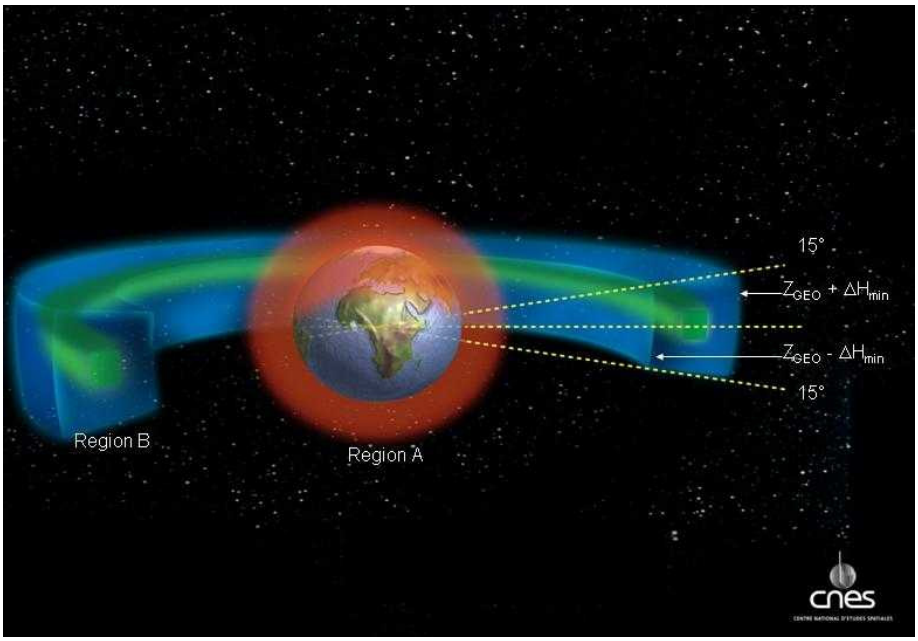

Figure 3.1. Three-dimensional view of geosynchronous ring

(Courtesy of Centre National d'Etudes Spatiales)

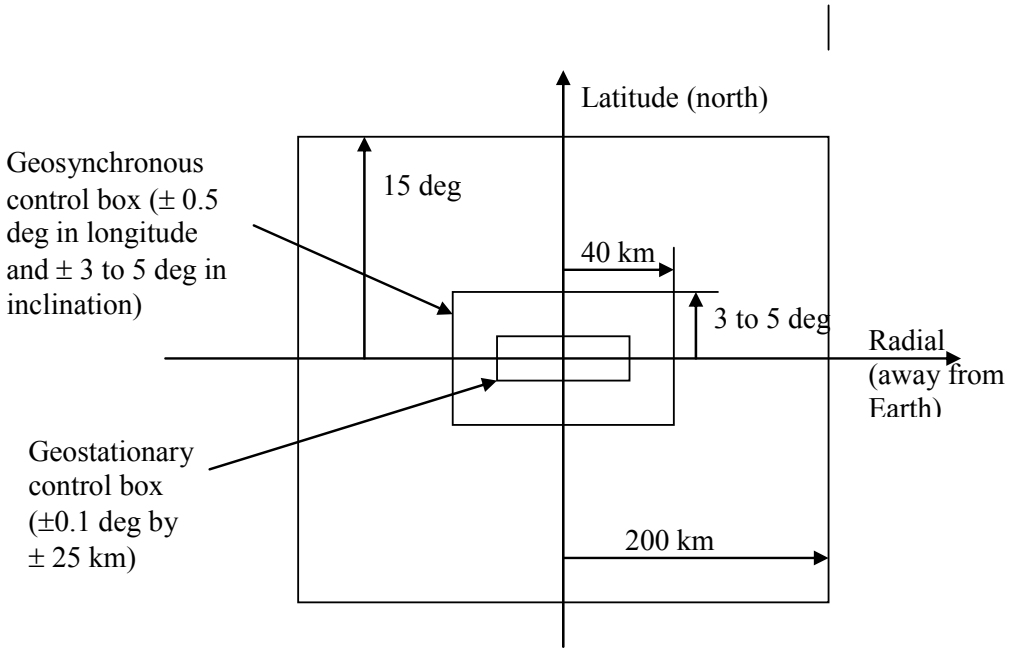

Figure 3.2. Cross section of the geosynchronous ring (not to scale).

3.4 Protected Region

The GEO protected region defined by the InterAgency Space Debris Coordinating Committee (IADC), as indicated by Region B in Fig. 4.1, includes the spherical shell centered on geostationary altitude with extent 200 km above and below this altitude and with inclination limits of +15 to – 15 degrees. While operations are usually conducted within about 75 km of geostationary altitude, the GEO protected region is extended in altitude to create a maneuver corridor for relocating spacecraft. Passivation of the disposed spacecraft is necessary to ensure that accidental explosions from on-board energy sources do not create debris that could reenter the protected region.

3.5 Re-orbit Maneuver

The action of moving a spacecraft to a new orbit.

4. Symbols and Acronyms

ω = argument of perigee of GEO disposal orbit
μ = Earth gravitational constant = 398600.4418 km^3/sec^2
Ω = RAAN = right ascension of ascending node of GEO disposal orbit
ΔH = change in altitude
ΔV = delta velocity or total velocity change
a = semi-major axis of GEO disposal orbit
A/m = area-to-mass ratio of spacecraft (projected area normal to Sun's rays)
C_R = index of surface reflection of the spacecraft ($0 < C_R < 2$)
e = eccentricity of GEO disposal orbit
i = inclination of GEO disposal orbit
h_{pmin} = minimum perigee altitude
L_S = solar longitude
M = mean anomaly of GEO disposal orbit
$p = a(1-e^2)$, *semilatus rectum* or semiparameter
r = radius of orbit
v = true anomaly

CDR	Critical Design Review
CNES	Centre National d'Etudes Spatiales
deg	degree
DoD	Department of Defense
EGM	Earth Gravity Model
EOMDP	End of Mission Disposal Plan
ESA	European Space Agency
FAA	Federal Aviation Administration
FCC	Federal Communications Commission
GEO	Geosynchronous or geostationary orbit
IAA	International Academy of Astronautics
IADC	InterAgency Space Debris Coordination Committee
I_{sp}	specific impulse (units of seconds)
ITU	International Telecommunications Union
JAXA	Japan Aerospace Exploration Agency
kg	kilogram
m	meter
NASA	National Aeronautics and Space Administration
PDR	Preliminary Design Review
rev	revolution
ROSCOSMOS	Russian Federal Space Agency
sec	second

5. Primary Requirements

5.1 Disposal Maneuver Planning

An "End of Mission Disposal Plan" (EOMDP) shall be developed, maintained, and updated in all phases of mission and spacecraft design and operation. This document shall include:

- Details of the nominal mission orbit
- Details of the targeted disposal orbit
- Estimates of the fuel required for the disposal action
- Identity of systems and capabilities required for successful completion of the disposal action
- Criteria that dictate initiation of the disposal action when met
- Identities of energy sources that must be depleted prior to end-of-life.
- A timeline for initiation and execution of the disposal action.
- A timeline for depletion of remaining energy sources
- A list of those individuals and/or entities to be notified of the end-of-mission and disposal and a timeline for notification.

5.2 Reliability for Disposal

The space system shall be designed such that the probability of successful end-of-mission disposal, including depletion of energy sources, exceeds 0.90. Details of the design that provides the basis for the probability estimate shall be included in the EOMDP.

5.3 Criteria for Executing Disposal Action

Specific criteria for initiation of the disposal action shall be developed, included in the EOMDP, and monitored throughout the mission life. Projections of mission life based on these criteria shall be made as a regular part of mission status reviews during the mission. The status of these criteria shall be presented at periodic (at least yearly) mission reviews.

5.4 Depletion of Energy Sources

Independent of the success or failure of other aspects of the disposal action, a contingency plan shall be developed to deplete all energy sources and safe the vehicle prior to the final demise of the spacecraft. The objective shall be to assure that actions necessary to safe the vehicle are taken before critical systems are lost. The contingency plan shall include criteria that define when the safing actions must be taken, the rationale for each criterion, and a schedule for safing actions. The contingency plan shall be included in the EOMDP.

6. Disposal Planning Requirements

Planning activities for end-of-mission disposal shall start in mission design. Planning for the actual disposal action shall begin at least six months prior to the date of re-orbit maneuvers. The following steps shall be followed in all mission phases and shall be documented in the EOMDP:

6.1 Develop an Accurate Estimate of the Fuel Reserves in the Propulsion System.

A minimum of 12/m/sec in ΔV capability (3-σ) shall be maintained for end-of-life orbit disposal. For a spacecraft mass of 2000 kg, the 12 m/sec velocity change translates into 8.1 kg of fuel at 300 sec I_{sp}.

6.2 Compute the Initial Perigee Increase.

The perigee altitude increase (in km) shall be computed as follows:

$$\Delta H = 235 + 1000 \cdot C_R \cdot A/m \qquad (6.1)$$

where C_R is the surface index of reflection ($0 < C_R < 2$), A/m is the spacecraft area-to-mass ratio in m^2/kg. The minimum value of C_R for computing initial perigee increase shall be no less than 1.5. Justification must be provided for using a value different than 1.5. Equation (7.1) was derived to ensure that the long-term perturbations will not cause the GEO debris to reenter a protected zone of GEO+200 km.

The minimum perigee altitude (in km) shall be computed as follows:

$$h_{pmin} = 36{,}021 \text{ km} + (1000 \cdot C_R \cdot A/m) \qquad (6.2)$$

This formula is based on a GEO altitude of 35,786 kilometers and establishes a "protected region" of 200 kilometers around GEO, plus 35 kilometers to account for the maximum descent of a re-orbited spacecraft due to lunar, solar, and geopotential perturbations.

6.3 Develop basic maneuver requirements for stable disposal orbit.

The final disposal orbit shall be stable; i.e., the perigee shall remain above the protected region for at least 100 years. This usually requires that the initial disposal perigee point towards the Sun and that the disposal maneuver be performed in the most favorable season of the year (it should be noted that the true optimal direction will differ slightly from the actual Sun-pointing direction due to lunar perturbations). See Appendix D for the optimal eccentricity and argument of perigee as a function of time for various solar reflectivity coefficients. Disposal orbits defined in accordance with the Equation 7.2 are stable if the final eccentricity is less than 0.003.

6.4 Verify long-term (100-year) disposal orbit characteristics.

Orbit propagation results using a reliable orbit propagator, either semi-analytic or numerical, shall be used to predict histories of perigee heights above GEO for a period of 100 years after initial insertion into the disposal orbit. The orbit propagator shall be of high precision and include as a minimum the perturbing forces of Earth's gravitational harmonics (up to a degree/order of 6 by 6), lunisolar attractions and solar radiation pressure. The precision of long-term propagation of

the propagator shall be verified against another well-established orbit propagator. Details on the orbit propagator used, assumptions made, and analysis results shall be included in the EOMDP.

6.5 Determine the maneuver sequence.

The maneuver sequence that will place the GEO spacecraft in the required disposal orbit with the optimal near Sun-pointing perigee and that will exhaust all the propellant onboard shall be determined. The disposal orbit is obtained after passivation and complete tank depletion, which can have unpredictable effects on orbit parameters and altitude. See Appendix A for examples. The initial conditions of the disposal orbit shall be determined using the steps outlined in paragraphs 7.3 and 7.4.

6.6 Develop a Vehicle Safing Plan.

This plan shall specify steps to be taken to deplete on-board energy sources after the satellite has been placed into the disposal orbit and shall include specific criteria for when the plan will be executed and a timeline to be followed. The Safing Plan shall include the possibility that failure of critical systems may dictate that safing actions be executed at any time during the mission or disposal action

6.7 Develop Contingency Plan.

In the event of a malfunction or other circumstance making it impossible to place the spacecraft into the final disposal orbit, a contingency plan shall be developed that includes

- Plans for selecting an alternative orbit that has as low a probability of future interference with operating satellites as possible (see Appendix C). The Contingency Plan shall include criteria and techniques to be used in the selection of this alternative orbit.
- Plans for maneuvering the satellite to the alternative orbit
- Plans for safing the satellite after the move to the alternative orbit.
- Plans for safing the vehicle should specify criterion be met at any time in the mission.

See Appendix C for an example where the quantity of propellant remaining is uncertain.

7. References

1. IADC-02-01, Revision 1, *Inter-Agency Space Debris Coordination Committee Mitigation (IADC) Guidelines* (Sep 2007)

2. FCC 04-130, Second Report and Order In the Matter of Orbital Debris, released 21 June 2004, Washington, D.C.

3. Chao, C.C, W.S. Campbell, G.E. Peterson, and W.H. Ailor, "Requirements for End-of-Life Disposal of Satellites Operating at Geosynchronous Altitude," Aerospace TOR -2006(8583)-4474, 3 November 2005

4. Campbell, W.S., "SMC Space Debris Mitigation Handbook Revision 2.0," Aerospace Report, TOR-2007(8506)-6693, 30 June 2007

5. ISO TC 20/SC 14 N, Space systems --- Disposal of satellites operating at geosynchronous altitude, 13 May 2009.

Appendix A: Optimal Maneuver Sequences

Two types of maneuver sequences are suggested depending on whether the orbit perigee is Sun-pointing or not at the end of operational life. Actual planning should consider mission constraints and uncertainties of fuel estimation.

The two main criteria for the maneuver sequence planning are: 1) ensure Sun-pointing or keep final orbit eccentricity small (less than 0.003) and 2) ensure all on-board energy sources are depleted or passsivated at the end of maneuvers.

Type A Maneuver Sequence — In this example, the initial perigee is already in the optimal direction, near-Sun-pointing, and a higher perigee increase than the minimum required 235 km is assumed. This sample maneuver sequence provides an adequate perigee increase for cases where some GEO customers may reserve more propellant than the minimum amount required. It is also anticipated that the current minimum required perigee increase of 235 km will eventually be changed to a higher value to redistribute the debris population density above the 200 km protected region.

Assuming an initial eccentricity of 0.0005 and the target perigee is 300 km above GEO, the following actions should be taken:

1. Perform first burn at apogee to raise perigee to GEO+200 km (ΔV= 4.0 m/sec).
2. Perform orbit determination two orbits later to obtain new orbit conditions.
3. Perform second burn at new apogee to raise perigee to GEO+300 km (ΔV= 5.0 m/sec).
4. Perform orbit determination two orbits later to obtain new orbit conditions.
5. Perform third burn at new apogee to raise perigee to GEO+250 km (ΔV= 0.9 m/sec and e = 0.000589).
6. Perform orbit determination at two orbits later to obtain new orbit conditions.
7. Perform fourth burn at perigee to raise apogee to GEO+350 km if propellant is available (ΔV= 0.9 m/sec and e = 0.00118).
8. Perform orbit determination at 1 and ½ orbits later to obtain new orbit conditions.
9. Perform fifth burn at apogee to raise perigee to GEO+300 km (ΔV= 0.9 m/sec and e = 0.000588).
10. Perform orbit determination at two orbits later to obtain new orbit conditions.
11. Perform sixth burn at apogee to raise perigee to GEO+325 km if adequate propellant is available (ΔV= 0.45 m/sec and e = 0.000294).
12. Continue to raise perigee and apogee by small increments (25 km or less) for each additional burn until propellant tanks are empty and keep perigee Sun-pointing as shown in the last two rows in Table A.1. The last few burns should be small and well planned such that the final eccentricity vector is as close to the optimal vector (see Appendix D) as possible.

Table A.1. Orbit Conditions and ΔV Consumed after Each Burn (Type A)

Burn number	Perigee ht. above GEO, km	Apogee ht. above GEO, km	Accumulated longitude drift, deg west	Eccentricity	ΔV, m/sec (accumulated)	Sun-pointing?
1	21	200	0	0.00212	4.0 (4.0)	No
2	200	300	3.2	0.00117	5.0 (9.0)	Yes
3	250	300	11.2	0.000589	0.9 (9.9)	Yes
4	250	350	20.0	0.00118	0.9 (10.8)	Yes
5[a]	300	350	27.6	0.000588	0.9 (11.7)	Yes
6	325	350	35.9	0.000294	0.45 (12.15)	Yes
7	325	375	44.5	0.000592	0.45 (12.6)	Yes
8	350	375	55.6	0.000296	0.45 (13.05)	Yes

[a] The minimum perigee increase, ΔH, computed by Eq. 7.1 can usually be satisfied after the fifth burn. The remaining burns are used to increase altitude until the propellant is exhausted (ΔV_T = 13.05 m/s, the assumed total ΔV remaining for orbit disposal).

The actual maneuver sequence should consider the ground-station-viewing constraint as the satellite is gradually drifting westward as shown in the fourth column of A.1. It may be two to three months before the last two to three burns (burns #6 to #8) can be performed. The estimated propellant mass to achieve a minimum perigee increase of 280 km is about 8 kg for a 2000 kg spacecraft with a chemical propulsion system (I_{sp}=300 sec).

Type B Maneuver Sequence — Initial perigee is not along the optimal direction (near Sun-pointing)

When the initial perigee is not Sun-pointing, the long-term eccentricity variation will be more pronounced and the minimum perigee altitude will be lower than the desired value of 300 km. The standard reorbit strategy is to execute the first two to three burns away from perigee or apogee to change the argument of perigee or the eccentricity vector. The change can be achieved without additional propellant or burns. Figure A.1 gives an example of induced change in argument of perigee versus the burn location on the orbit.

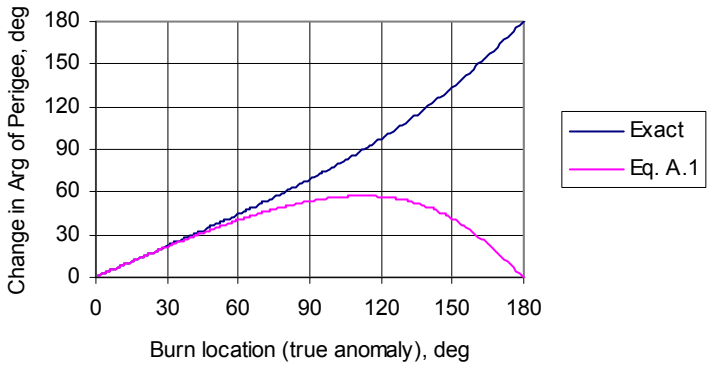

Figure A.1. Induced change in argument of perigee vs. burn location.

The example assumes an initial eccentricity of 0.0005 and the magnitude of the ΔV is 2.0 m/s. This burn will also raise the semi-major axis by the desired amount, about 55 km. The top curve is computed from equations based on closed form orbit relations to be discussed in Appendix B. The bottom curve is computed from the simplified linear relations shown below.

$$\Delta e = (\Delta a/a) \cos v \qquad (A.1)$$

$$e\Delta\omega = (\Delta a/a) \sin v$$

where Δe and Δω are the induced changes in eccentricity and argument; Δa is the planned increase in mean orbit altitude or semi-major axis; and the angle v is the true anomaly where a single burn is executed. The eccentricity in front of Δω on the left hand side of the equation is the new eccentricity after the burn. Fig A.1 shows that the simplified relations for determining the induced change in argument of perigee give good approximations when the burn location (true anomaly), central angle from perigee, is less than 90 deg. The above simplified relations are useful in the initial design of the Type B maneuver sequence for orbits whose perigee is not Sun-pointing.

Figure A.2 shows the corresponding change in eccentricity. The approximate relation (Eq. A.1) is good for eccentricity computation when the true anomaly is less than 40 deg.

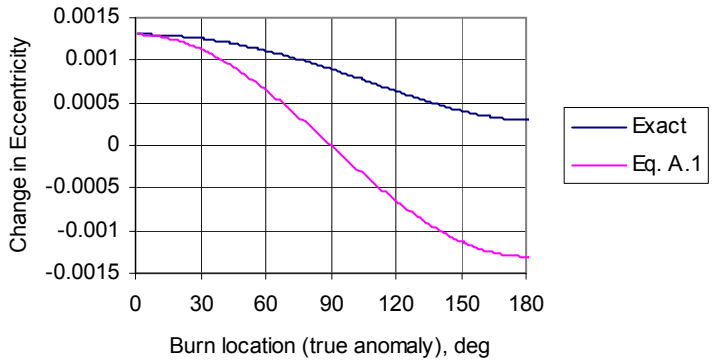

Figure A.2. Induced change in eccentricity vs. burn location (e_0=0.0005, ΔV=2.0 m/s).

When the perigee becomes Sun-pointing after the first two or three burns, the remaining burn sequence should follow the Type A maneuver sequence.

Sample Maneuver Sequence

A sample maneuver sequence is illustrated below assuming a 70 deg difference between the initial perigee and the Sun vector (Sun is 70 deg east of perigee vector).

1. Perform first burn at 60 deg past perigee or true anomaly = 60 deg with a ΔV of 2.0 m/sec along the intrack direction to raise orbit altitude.
2. Perform orbit determination at one or two orbits later to obtain new orbit conditions. The new orbit should be: a = 42220.86 km, e = 0.001613, same inclination and RAAN, argument of perigee advanced by 44.42 deg.

3. Perform second burn at 56 deg past the new perigee with a ΔV of 2.0 m/sec along the intrack direction.
4. Perform orbit determination at one or two orbits later to obtain new orbit conditions. The new orbit after the second burn should be Sun-pointing with a = 42275.96 km, e = 0.002584, and argument of perigee advanced by another 25 deg.
5 Perform third burn at new apogee to raise perigee to GEO+250 km (ΔV= 4.52 m/sec and e = 0.000362).
6. Perform orbit determination at two orbits later to obtain new orbit conditions.
7. Perform fourth burn at new apogee to raise perigee to GEO+325 km (ΔV= 1.91 m/sec and e = 0.0008833).
8. Perform orbit determination at two orbits later to obtain new orbit conditions.
9. Perform fifth burn at apogee to raise perigee to GEO+300 km (ΔV= 0.9 m/sec and e = 0.000294).
10. Perform orbit determination at two orbits later to obtain new orbit conditions.
11. Perform sixth burn at perigee to raise apogee by 50 km if propellant is available (ΔV= 0.9 m/sec and e = 0.000872).
12. Repeat 7 and 8 to raise perigee by 25 km (ΔV=0.45 m/sec) after each additional burn and continue until propellant tanks are empty.

Table A.2. Orbit Conditions and ΔV Consumed after Each Burn (Type B)

Burn number	Perigee ht. above GEO, km	Apogee ht. above GEO, km	Accumulated longitude drift, deg west	Eccentricity	ΔV, m/sec (accumulated)	Sun-pointing?
1	-13	123	0	0.001613	2.0 (2.0)	No
2	1	219	1.74	0.002584	2.0 (4.0)	Yes
3	219	250	4.55	0.000362	4.52 (8.52)	No
4	250	325	10.5	0.000893	1.91 (10.43)	Yes
5	300	325	18.0	0.000294	0.9 (11.33)	Yes
6	300	375	26.0	0.000872	0.9 (12.23)	Yes
7	325	375	34.6	0.000592	0.45 (12.68)	Yes
8	350	375	43.5	0.000296	0.45 (13.13)	Yes

The actual maneuver sequence should consider the ground-station-viewing constraint as the satellite is gradually drifting westward as shown in the fourth column of A.2. It may be two to three months before the last two to three burns (burns #6 to #8) can be performed. The estimated propellant mass to achieve a minimum perigee increase of 280 km is about 8 kg for a 2000 kg spacecraft with a chemical propulsion system (I_{sp}=300 sec).

Appendix B: Example Calculations

Closed Form Equations for Computing Off-Perigee Burn Locations

When a reorbit burn is applied at a location away from perigee or apogee, changes in argument of perigee and eccentricity occur. The magnitude and direction of the changes depend on burn vector and location of the burn.

In this application, the single-burn vector is assumed along the intrack direction or perpendicular to the radial direction. The burn is assumed impulsive. The computation starts with a given ΔV applied at a given location on the orbit with true anomaly, v_0. The following Keplerian relations will lead to the induced eccentricity and argument of perigee.

From vis-viva integral, the new semi-major axis, a, is computed after the ΔV is applied at a given true anomaly, v, and the total orbit velocity after the burn is $V= V_0+\Delta V$:

$$a = 1/(2/r - V^2/\mu) \tag{B.1}$$

where V_0 is orbit velocity before the burn, r is the radius of the orbit at the time of burn and μ is the Earth gravitational constant. One Keplerian relation gives:

$$e \cos v = p/r - 1 = a(1-e^2)/r - 1 \tag{B.2}$$

assuming that the ΔV is along the intrack direction and the velocity component in the radial direction is not affected. Therefore,

$$e \sin v = (\mu/p_0)^{1/2} (p/\mu)^{1/2} e_0 \sin v_0 = (p/p_0)^{1/2} e_0 \sin v_0 \tag{B.3}$$

where $p=a(1-e^2)$ and $p_0=a_0(1-e_0^2)$; the elements with a subscript "0" are the elements before the burn. Equations B.2 and B.3 can then be used to solve for e and v by iteration through:

$$e^2 = (e \sin v)^2 + (e \cos v)^2 \tag{B.4}$$

$$v = \tan^{-1} [(e \sin v)/(e \cos v)]$$

After knowing the true anomaly, v, the new value of argument of perigee is

$$\omega = v_0 + \omega_0 - v \tag{B.5}$$

With the above procedure, the desired burn location, v_0, can be determined by iteration.

Sample 100-Year Histories of Sun-Pointing Disposal Orbits

A Sun-pointing geometry is selected by assuming an epoch of 1 July 2018. Figure B.1 illustrates the Sun-pointing geometry of this example. A midnight-pointing perigee would be achieved for the same initial orbital elements by changing the epoch to 1 January 2018.

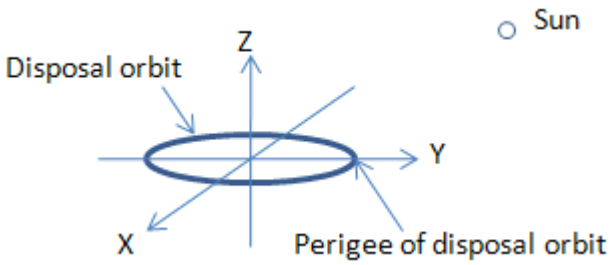

Figure B.1. Sun-pointing geometry with 1 July epoch.

The sample orbital elements of a GEO disposal orbit for 100-year integration are determined from the assumed initial eccentricity of 0.0005 with A/m = 0.035 m^2/kg and C_R = 1.3. The recommended altitude increase is

$$\Delta H = 235 + 1000 \times C_R \times A/m \qquad (B.6)$$
$$= 235 + 1000 \times 1.3 \times (0.035)$$
$$= 280.5 \text{ km}$$

The corresponding semi-major axis is 42467.6 km, e= 0.0005, i = 0.1 deg, Ω = 90 deg, ω = 0 deg, and M = 0 deg. A high-precision N-body numerical integration tool was employed to generate all the long-term orbit results presented in the following figures. The perturbing forces included are: Earth gravity harmonics (6x6 EGM 96), lunisolar attractions and solar radiation pressure.

Figure B.2 shows the perigee height history of the 100-year integration. The perigee height history is well behaved with perigee never below GEO+250 km. However, when the perigee is pointing to the local midnight, a much larger oscillation in perigee height is found in the 100-year integration (Fig. B.3). The minimum perigee height above GEO is approaching 200 km. This finding clearly suggests that the reorbit insertion should be performed with perigee pointing to the Sun. A long-period variation with a period of about 10.5 years, caused by Sun/Moon attractions, is apparent in these two cases (Figs B.2 and B.3) as well as the other 100-year eccentricity histories.

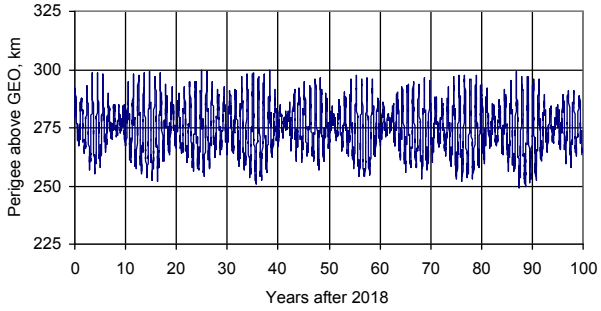

Figure B.2. 100-year perigee history (Sun-pointing).

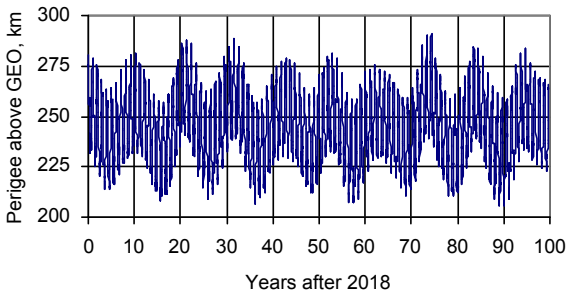

Figure B.3. 100-year perigee history (point to midnight).

Several cases of 100-year integration were repeated to study the sensitivity of perigee height to epoch. The initial orbit elements are the same as before for each case at July 1 or January 1 of each epoch year. In each 100-year integration, only the minimum perigee height above GEO is recorded and plotted as in Figure B.4. The upper curve represents the minimum perigee height for July 1 epoch (Sun-pointing), and the lower curve represents the minimum perigee height for January 1 epoch (perigee pointing to midnight). The epoch is varied from January 1, 2005 to July 1, 2025. Figure B.4 shows the sensitivity to epoch.

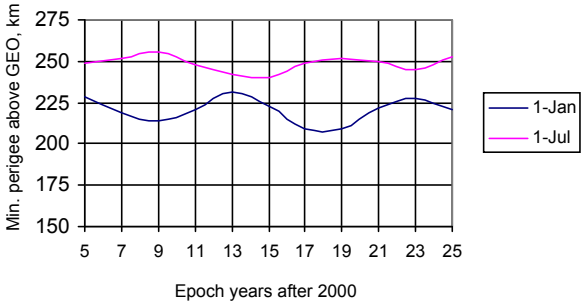

Figure B.4. Minimum perigee height vs. epoch.

To determine whether there is a seasonal variation, the 100-year integration is repeated only for the Sun-pointing case (upper curve in Fig.B.4) on the first day of each month for four selected years (2005, 2009, 2014 and 2018). Figure B.5 shows the seasonal variation of the minimum perigee heights. The four curves in Fig B.5 reveal another interesting fact that the peak of the seasonal variation changes to a valley in about every 4 years, or one-fourth of the 18.6-year lunar cycle. The same trend can be seen in Figure B.4 where the peaks occur in summer (July 1) for 2009 and 2018.

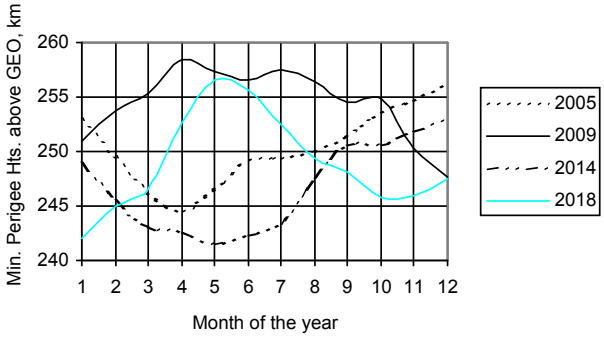

Figure B.5. Minimum perigee height vs. month of the year.

This finding reveals that the recommended altitude increase (280.5 km) yields a minimum perigee of 250 km or higher for 100 years if the orbit insertion is performed near the peak season (Figs.B.4 and B.5) following Sun-pointing geometry. For example, if a disposal orbit maneuver sequence is to be planned in 2009, the best time for the reorbit to take place is sometime in April, as indicated in Figure B.5.

When the perigee is pointing to a direction away from the Sun or toward midnight, the minimum perigee height obtained from the 100-year integration changes. Figure B.6 shows the sensitivity to perigee pointing as a function of the combined angle, $\omega+\Omega$, for two epochs. On July 1, the Sun-pointing geometry occurs when $\omega+\Omega$ is 90 deg. On January 1, the Sun-pointing geometry occurs when $\omega+\Omega$ is 270 deg. The results clearly show that highest value of minimum perigee height occurs when perigee is Sun-pointing.

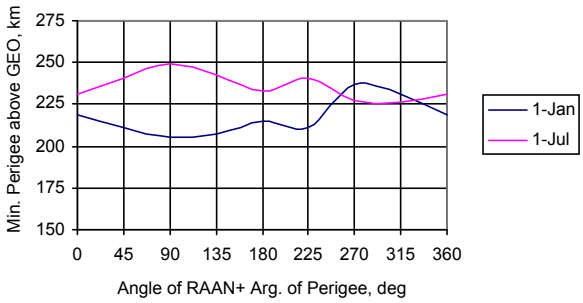

Figure B.6. Minimum perigee height vs. ($\omega+\Omega$).

Figure B.7 shows the minimum perigee height above GEO determined from 100-year integration versus the initial eccentricity of the disposal orbit. The same set of initial orbital elements is assumed with two epochs, 1 July and 1 January 2018. All the cases satisfy the initial perigee altitude increase, ΔH, determined by Equation B.6 (280.5 km).

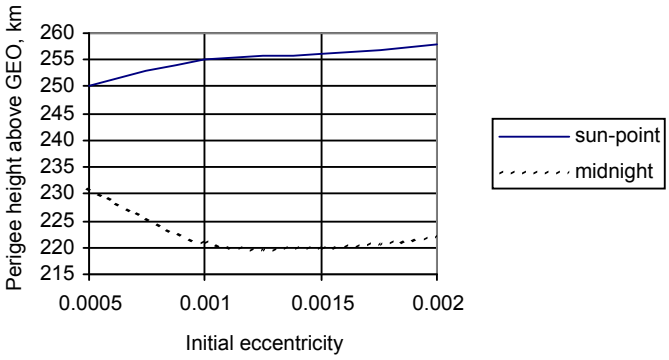

Figure B.7. Minimum perigee height above GEO vs. initial eccentricity.

The results indicate that smaller eccentricity at 0.0005 tends to keep the minimum perigee higher at 230 km when the perigee is pointing to midnight (dashed curve in Fig B.7). The results also show that larger initial eccentricity actually increases the minimum perigee height if the Sun-pointing geometry is followed (solid curve in Fig B.7). However, larger initial eccentricity with the same initial perigee altitude increase (280.5 km) requires more fuel, which is undesirable for mission operations. Figure B.8 gives an estimate of the ΔV requirement as a function of initial eccentricity of a GEO disposal orbit with initial altitude increase of 280.5 km.

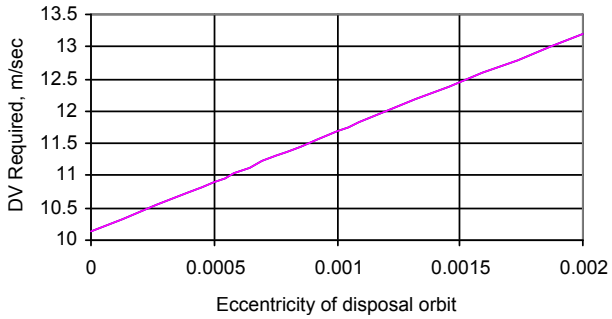

Figure B.8. ΔV required for reorbit vs. eccentricity.

As seen from the linear relation in Fig B.8, an initial eccentricity of 0.002 requires about 2.4 m/sec or 22% more ΔV than that for an eccentricity of 0.0005.

The uncertainties in the long-term prediction of perigee altitudes may be estimated from the uncertainties in predicting semi-major axis and eccentricity. The major source of error in predicting semi-major axis and eccentricity of a super-synchronous orbit comes from the uncertainty in modeling the solar radiation pressure that is proportional to the effective spacecraft area-to-mass ratio. Because of the uncertainty in determining the attitude of an inactive spacecraft, it is difficult to estimate accurately the effective area-to-mass ratio. In the 100-year predictions presented here, a constant effective A/m of 0.035 m^2/kg with a value of 1.3 for C_R is assumed for all cases. Numerical tests show that a 20% decrease in A/m will increase the minimum perigee height by about 5 km.

These sample plots show that long-term eccentricity or perigee stability of GEO disposal orbits can be significantly improved by having the initial perigee pointing to the Sun and performing the reorbit in the most favorable season of the year.

Appendix C: Disposal Strategy And Analysis For Sample Geo Satellite

Normally, a satellite at the end of its useful life is moved to a higher orbit with a minimum perigee ranging from 235 km to 300 km above GEO. Often the satellite is disposed of in a few maneuvers in order to get it out of the way as quickly as possible. However, there are times when the satellite being moved has an unknown amount of fuel or a questionable state-of-health. This implies that the vehicle could fail at any time and therefore relying upon a few large burns may not be the best way to get the largest clearance from the GEO belt over a long period of time.

Instead, a safer method of disposal is to target an optimal eccentricity and argument of perigee and try to conduct smaller burns in pairs approximately 12 (or 36) hours apart. In this manner, the 100-year perigee altitude behavior stays consistently higher than it otherwise would, possibly by up to 40-50 km for the same cost in ΔV. This significantly reduces the risk of collision between the disposed satellite and other operational vehicles in GEO. A sample case for a GEO satellite is examined below to show the net effect of the proposed strategy.

The pre-disposal conditions for the sample satellite were: eccentricity of 0.000317, 7.7 degrees in inclination, 62.3 degrees in RAAN, 353 degrees in argument of perigee, solar radiation coefficient (CR*A/m) of 0.0374 m2/kg, and an epoch of May 28, 2005. The satellite was assumed to be originally in GEO with a final desired disposal orbit at least 300 km above GEO.

A mean element propagator was used to generate 100-year time histories of the perigee altitude above GEO for a variety of initial conditions. The force models used were the 6x6 EGM96 gravity field, solar radiation pressure, and solar and lunar perturbations.

Sweeping over the entire range of argument of perigee from 0 to 360 degrees for various eccentricities and saving the minimum perigee altitude over 100 years from each run gives Figure C.1. Once again, the initial inclination and node were 7.7 and 62.3 degrees, respectively, with a semi-major axis of 160 km above GEO. The argument of perigee increment was 5 degrees; the eccentricity increment was 1x10-4. For this sample case, the optimal argument of perigee was approximately 20 degrees; the worst argument of perigee was at 200 degrees. The Sun-pointing strategy would imply an argument of perigee of about 5 degrees; the true optimal is thus somewhat different than the Sun-pointing angle. It is seen from this plot that the optimal point is strongly dependent on the initial argument of perigee and weakly dependent upon the eccentricity. The difference between the highest and lowest minimum perigee is over 50 km for the same eccentricity, implying that targeting the optimal argument of perigee is very important to a successful disposal strategy.

Figure C.2 shows the eccentricity dependency at the optimal argument of perigee of 20 degrees. The same initial conditions were used as in Figure C.1, but a finer resolution in the eccentricity of 2.5x10-5 was utilized to get a more accurate result. For this satellite, the preferred target eccentricity was about 0.000590. It should be noted that the nominal Sun-pointing strategy implies a target eccentricity of only 0.000374 (0.01 x solar coefficient). However, as will be shown next, the solar and lunar perturbations contribute to the value of the eccentricity along with the solar radiation pressure causing the higher target value.

The burn plan should then be to perform burns such that the post-burn eccentricity and argument of perigee are kept as close to the target values as possible. From Figures C.1 and C.2, there is an allowable tolerance of ~ +10 degrees in argument of perigee and +0.00016 in eccentricity to maintain a minimum perigee altitude within 5 km of the maximum value. These are well within

the targeting capabilities of GEO satellites. It should be stressed that these values apply only to the sample case as set forth here. Differing initial conditions, especially the node, epoch, and solar radiation coefficient, will change the optimal values (as will be shown later, the semi-major axis and inclination contribute little to the optimal values of the argument of perigee and eccentricity).

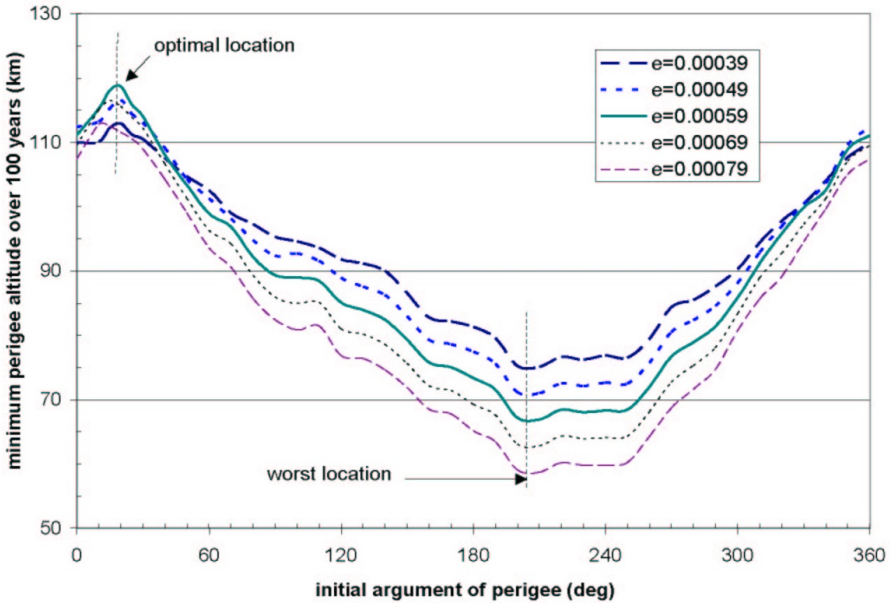

Figure C.1. Dependency of minimum perigee altitude on argument of perigee.

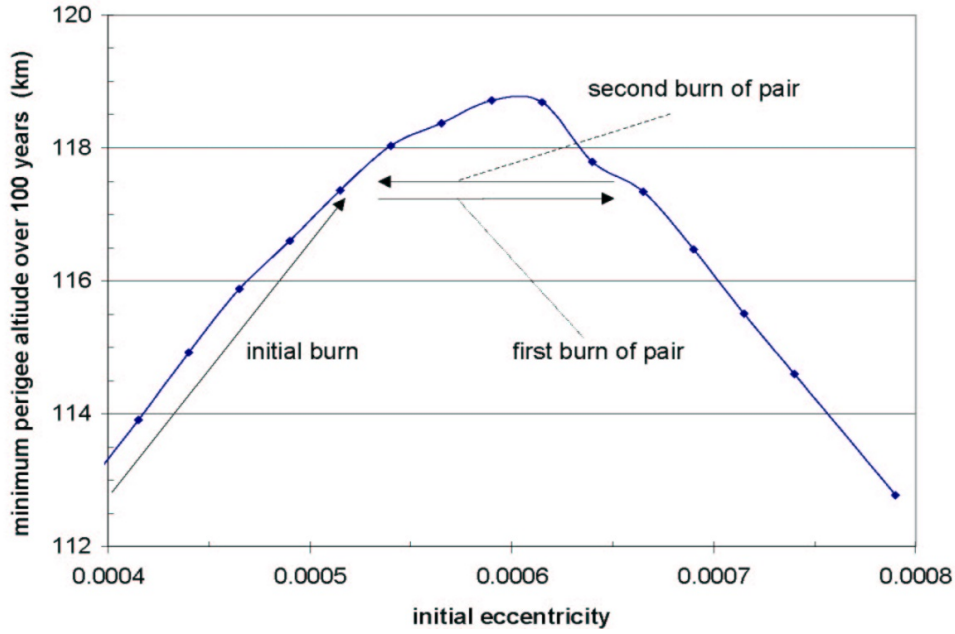

Figure C.2. Dependency of minimum perigee altitude on eccentricity.

As an example burn profile, (also shown in Figure C.2), the initial burn would be to increase the eccentricity from the pre-disposal value of 0.000317 to 0.00052 while moving the argument of perigee to within 10 degrees of the target value of 20 degrees. Then subsequent burns would take place in pairs with the first burn of the pair to increase the altitude and raise the eccentricity to 0.00065 while keeping the argument of perigee close to 20 degrees. The second burn of the pair would also raise the altitude but would decrease the eccentricity back to 0.00052 and so on until the desired change in altitude is accomplished. In essence, the satellite is "walked" up to the desired disposal altitude. If a failure occurred at any point in time, then the satellite is guaranteed of achieving the best possible clearance over the next 100 years.

Figure C.3 shows the dependency of the minimum perigee altitude over the next 100 years broken down by the type of perturbation for the optimal eccentricity of 0.000590. It is seen that the gravity field alone (empty circles in Figure C.3) does not contribute very much to the argument of perigee dependency; neither does the solar gravitation (asterisks). Instead, the solar radiation pressure (squares) and the lunar perturbation (solid circles) act together to create the results for the combined perturbations (solid line). It is important to note that the solar radiation pressure optimal argument of perigee is at about 5 degrees, given the epoch of May 28, 2005 (solar longitude of 66 degrees) and the initial right ascension of ascending node (RAAN) of 62 degrees, which implies that the orbit would be very near the Sun-pointing orientation (argument of perigee plus RAAN = solar longitude). However, the presence of the lunar perturbations causes the final optimal point to deviate from the ideal Sun-pointing strategy. Additional runs performed at epochs 4 months and 8 months later confirmed these results.

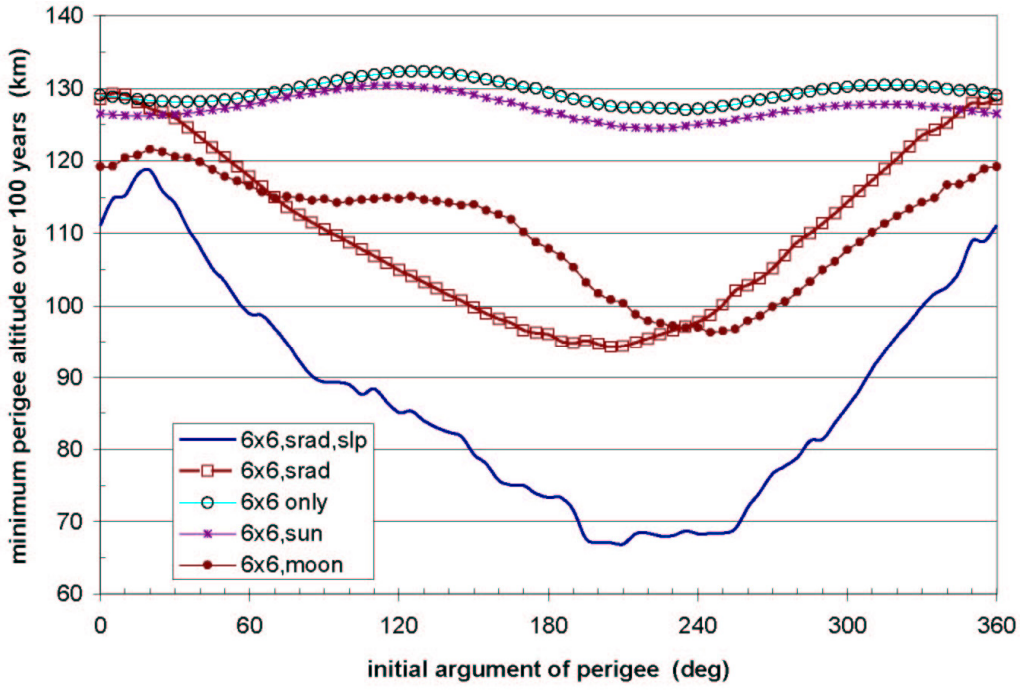

Figure C.3. Contribution of individual perturbations.

Once the optimal eccentricity and argument of perigee have been established, the question is how sensitive are the target values to changes in the semi-major axis (i.e., as the satellite moves higher during the maneuver sequence do the optimal values change in any significant way?). Runs were

performed to find the optimal argument of perigee and eccentricity for varying semi-major axis while keeping the node and epoch constant. This was also performed for varying inclinations to determine the sensitivity to that orbit parameter. In neither case was there a significant change in the optimal values. However, when the semi-major axis was precisely at GEO altitude, the optimal values were noticeably different (e~0.0004904, ω~60 deg). This is due to the gravity field harmonics being in resonance at GEO altitude. Still, once the satellite moved even slightly above GEO (~50 km), the optimal eccentricity and argument of perigee settled down to consistent values.

After the initial burn is performed as shown in Figure C.1, how should the subsequent burn pairs be conducted? The usual assumption would be to burn in pairs at perigee and apogee in order to keep the argument of perigee constant. But Figure C.4 shows the effect of the timing of the burns in relation to each other. This plot was generated by assuming a first burn at a certain location in the orbit and then trying the second burn at separate 1 hour intervals over the next 24 hours. The x-axis shows the hours past perigee of the first burn (24 hours to one orbit at GEO so burns at both 0 and 24 hours are at perigee). There are two y-axes: the left hand axis (solid diamonds) show the subsequent minimum perigee altitude over the next 100 years for a given pair of burns while the right hand axis (open squares) shows the time of the second burn in relation to the first burn. The magnitude of the burns was 0.5 m/s.

For example, if the first burn of the pair is performed at perigee (0 hours), then 24 subsequent runs were performed at 1 hour, 2 hours, 3 hours, etc., after perigee. The highest (best) minimum perigee of the 24 runs was saved. In this case, the highest minimum perigee occurred when the second burn was at 12 hours past the first burn (point is denoted by the solid arrow and is associated with the right hand y-axis) and yielded a perigee altitude of 116.6 km (point is denoted by the dashed arrow and is associated with the left hand y-axis). As can be seen from this plot, the best burn pairing does not occur at perigee/apogee, but is actually almost 90 degrees away from that location. The deviation, however, is not much: only about 6 km from the peak to valley.

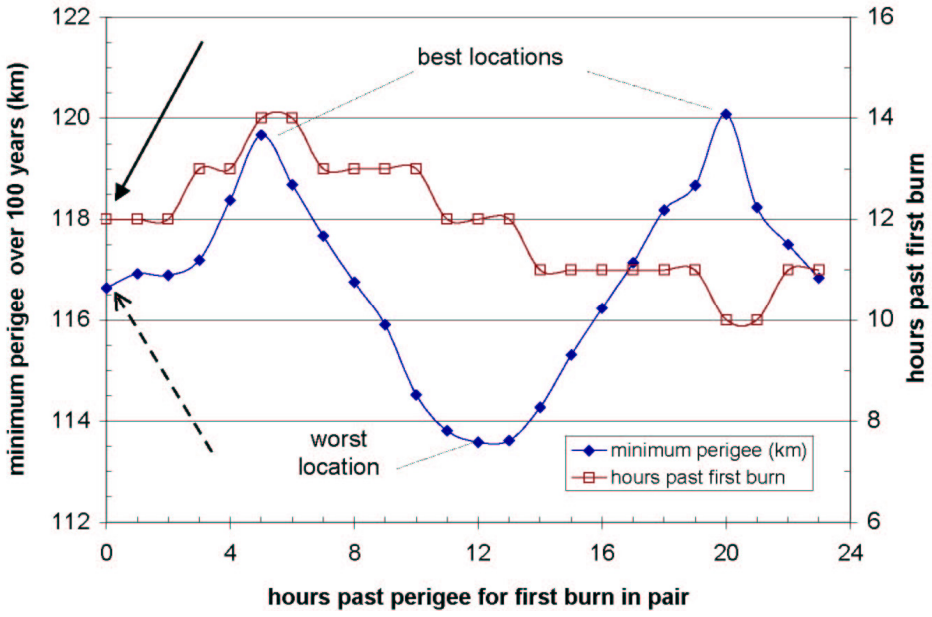

Figure C.4. Optimal locations in orbit for burn pair.

On the other hand, Figure C.5 shows several sample cases denoting the two best solutions from Figure C.4 at 5 and 20 hours along with the worst solution at 12 hours and the perigee (0 hour) solution. Here the variation is 30 km peak to valley. The conclusion from these two figures is that while there may be optimal times within a given orbit to conduct the burns, the benefit gained is not substantial (~6 km; Figure C.4). Instead, it is much more advantageous to conduct the burns roughly one-half of an orbital revolution apart (~30 km; Figure C.5). The bottom line is that keeping the burns half-a-rev apart is more important than where in the orbit the burns occur.

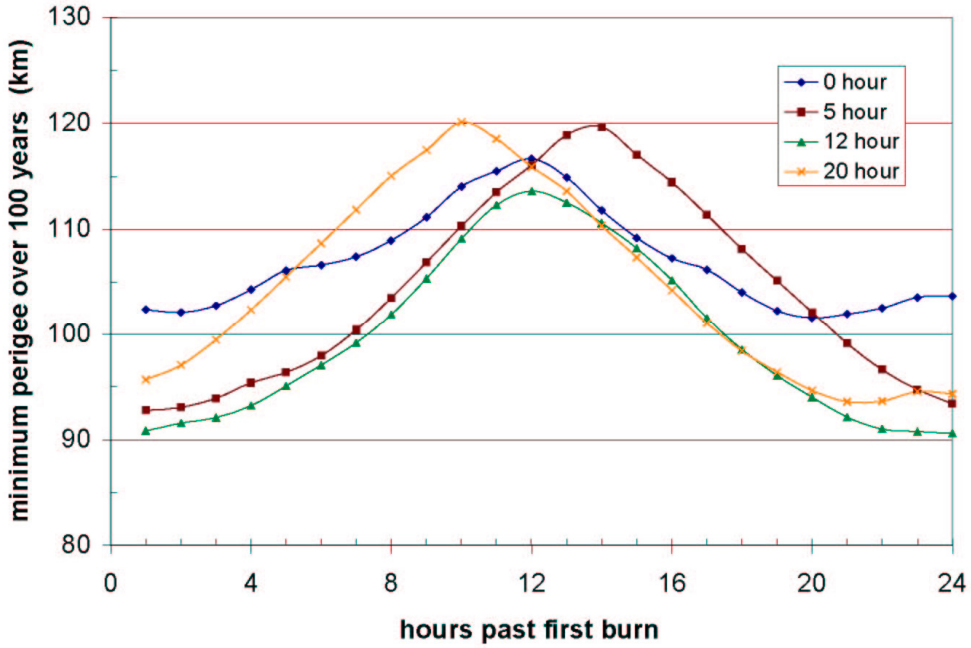

Figure C.5. Individual sample cases from Figure C.4.

The effectiveness of the proposed eccentric burn strategy is shown in Figure C.6 as a function of cumulative ΔV. Three burn profiles are given. The first is the proposed eccentricity control strategy where an initial 0.5 m/s burn is applied near perigee followed by a smaller 0.25 m/s burn 24 hours later to establish the orbit near the target e and ω. This is then followed by 0.5 m/s burn pairs about 36 hours apart conducted in such a way as to keep e and ω to within 0.00014 and 10 degrees of optimal, respectively. The circularization strategy assumes the original orbit (e=0.000317, =353 deg) and conducts burns of 0.5 m/s at apogee and perigee. In this manner, the original ω is maintained close to 353 deg. It is clear that the proposed eccentricity strategy results in a much more favorable clearance of the GEO belt than simple apogee-perigee burns. The worst profile is the apogee-perigee burn pairing coupled with an initial argument of perigee of 200 degrees. This situation should be avoided at all costs.

In conclusion, targeting the optimal eccentricity and argument of perigee during the disposal maneuvers can have a significant improvement in the 100-year clearance of the GEO belt as opposed to simply burning in the usual apogee-perigee manner. However, the results deriving from this study imply that while the Sun-pointing strategy is close to the true optimal argument of perigee and eccentricity, lunar perturbations will cause the optimal values to be slightly different than the pure Sun-pointing values. Therefore, the true optimal should be determined on a case-by-case basis.

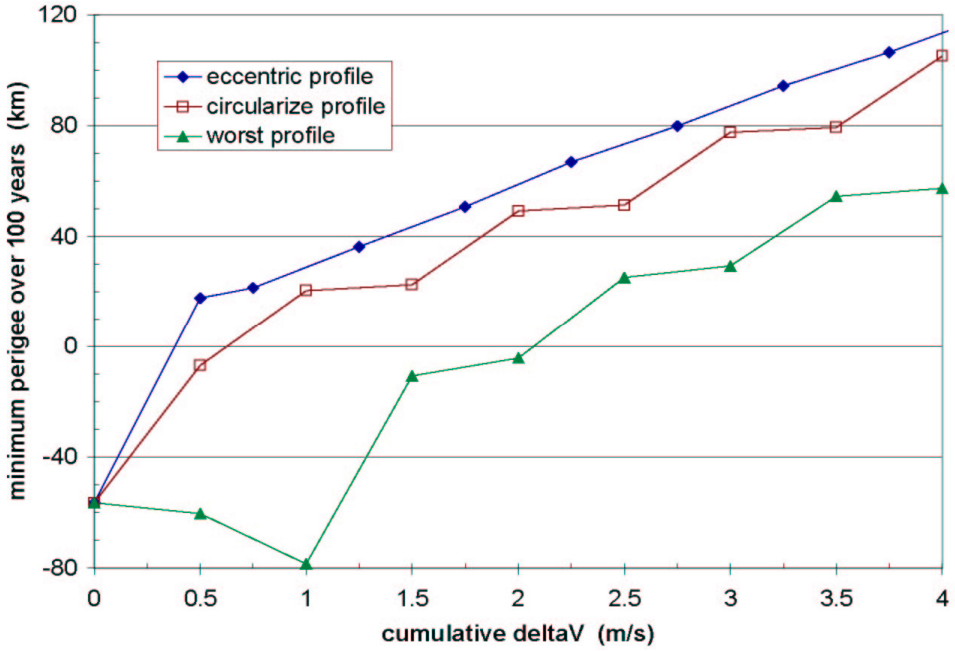

Figure C.6. Effectiveness of proposed strategy for sample GEO case.

Appendix D: Tabulated Values Of The Optimal Eccentricity Vector

The following tables contain the optimal eccentricity vector (eccentricity and argument of perigee plus RAAN (or longitude of periapsis)) as a function of time and a function of the solar reflectivity index (C_R x A/m in m^2/kg) that will yield the highest perigee over the next 100 years. The search to find the optimal values was performed in a brute force fashion in increments of 2.3×10^{-5} in eccentricity and 5 degrees in longitude of periapsis. The benefit gained from using the optimal vector over the Sun-pointing strategy varied from 0 to 20 km (average ~9 km). However, if the sun-pointing strategy is chosen for the disposed vehicle, then the longitude of periapsis should be set equal to the value of the solar longitude (depicted as L_S in the tables) with an eccentricity equal to $0.01 \times C_R \times$ A/m. These charts can be interpolated to find the optimal vector for any particular satellite at a given time. However, the following should be noted when using these tables.

The initial conditions used to generate the data assumed a constant semi-major axis of 300 km above GEO (i.e., a constant ΔV used in the disposal), mean anomaly of 180 deg (i.e., the last burn occurs at apogee raising the perigee so that the eccentricity is equal to the tabulated value), an inclination of 7.74 deg (maximum at end-of-life if inclination drift is allowed), and an epoch of 0:00 UT on the first day of each month. Additional analysis has shown that the optimal vector depends little upon these elements (the minimum perigee altitude may vary by ~2 km for each component), but if a high level of accuracy is required for a given disposal, the interpolated values found from the tables should be used as an initial guess in order to find the true optimal for a particular disposal situation. The exception is the RAAN: in the search process, the initial RAAN was set to 62.3 deg and the argument of perigee was changed in 5 deg increments until the optimal value was found. Different RAANs were then checked and it was found that the relevant angular parameter is the argument of perigee plus RAAN; if this value is held constant, then the results will again be consistent to 1-2 km irrespective of the particular RAAN.

In addition, care should be taken if performing interpolation on the values. It was found in conducting the optimal search in the angular argument that at times there was not one pure maximum, but multiple local maxima. As either the time or C_R x A/m advanced, the true maximum would jump from one peak to another.

For example, consider the May 01, 2008 disposal date. A C_R x A/m of 0.015 m^2/kg has an optimal eccentricity and longitude of periapsis of 0.00004 and 262.3 deg while the C_R x A/m of 0.03 m^2/kg has optimal values of 0.00009 and 37.3 deg. Linearly interpolating would imply optimal values of 0.000057 and 307.3 deg for a C_R x A/m of 0.02 m^2/kg. Instead, the C_R x A/m=0.02 optimal value was actually 0.000015 and 47.3 deg. In this case, the optimal point switched from one maximum to another, and therefore the intermediate maximum would actually be close to one or the other point.

Therefore, it is recommended that when confronted with angular changes of greater than 90 deg, interpolation should not be performed. Instead, the closer value should be used either directly or as a starting point for a more refined search.

A few final comments on the general behavior of the system are warranted. When the area-to-mass ratio was small (C_R x A/m < 0.01), the optimal angle was pointed at the lunar apogee; when the area-to-mass ratio was large (C_R x A/m > 0.03), the solar radiation pressure force became dominant and the optimal angle was directed towards the Sun.

Table D1. Optimal Eccentricity Vector for C_R x A/m = 0.00, 0.005 & 0.01 m^2/kg

Year	Mon	L_S (deg)	C_R x A/m = 0.00 m^2/kg eccen	$\omega+\Omega$	C_R x A/m = 0.005 m^2/kg eccen	$\omega+\Omega$	C_R x A/m = 0.01 m^2/kg eccen	$\omega+\Omega$
2006	1	281	0.000115	132.3	0.000065	142.3	0.000090	177.3
	2	314	0.000140	112.3	0.000115	102.3	0.000065	102.3
	3	341	0.000140	117.3	0.000115	117.3	0.000115	92.3
	4	10	0.000140	142.3	0.000115	132.3	0.000090	117.3
	5	38	0.000140	162.3	0.000115	147.3	0.000090	127.3
	6	68	0.000115	177.3	0.000115	167.3	0.000090	122.3
	7	99	0.000065	167.3	0.000090	122.3	0.000140	117.3
	8	131	0.000090	142.3	0.000140	137.3	0.000190	137.3
	9	160	0.000115	157.3	0.000165	157.3	0.000215	157.3
	10	187	0.000090	167.3	0.000140	172.3	0.000215	177.3
	11	216	0.000090	187.3	0.000140	202.3	0.000215	207.3
	12	246	0.000165	177.3	0.000115	207.3	0.000165	222.3
2007	1	281	0.000140	187.3	0.000140	207.3	0.000140	222.3
	2	314	0.000165	207.3	0.000165	217.3	0.000165	232.3
	3	341	0.000165	212.3	0.000115	227.3	0.000115	242.3
	4	10	0.000090	217.3	0.000065	237.3	0.000040	257.3
	5	37	0.000040	192.3	0.000015	167.3	0.000015	147.3
	6	68	0.000115	192.3	0.000090	172.3	0.000115	162.3
	7	99	0.000140	202.3	0.000165	192.3	0.000140	177.3
	8	130	0.000190	222.3	0.000165	212.3	0.000140	197.3
	9	159	0.000165	237.3	0.000165	222.3	0.000190	207.3
	10	186	0.000115	207.3	0.000165	212.3	0.000240	212.3
	11	215	0.000190	227.3	0.000240	227.3	0.000290	227.3
	12	246	0.000165	232.3	0.000215	237.3	0.000290	242.3
2008	1	280	0.000115	237.3	0.000165	252.3	0.000215	252.3
	2	313	0.000090	222.3	0.000115	247.3	0.000140	262.3
	3	342	0.000115	227.3	0.000090	252.3	0.000115	272.3
	4	10	0.000140	227.3	0.000115	242.3	0.000065	267.3
	5	38	0.000190	237.3	0.000115	242.3	0.000090	252.3
	6	69	0.000165	247.3	0.000115	247.3	0.000040	242.3
	7	100	0.000140	237.3	0.000115	227.3	0.000140	212.3
	8	131	0.000215	237.3	0.000240	232.3	0.000215	222.3
	9	160	0.000215	252.3	0.000165	242.3	0.000165	232.3
	10	187	0.000140	262.3	0.000165	247.3	0.000190	237.3
	11	216	0.000215	247.3	0.000115	252.3	0.000165	242.3
	12	247	0.000090	237.3	0.000140	242.3	0.000190	247.3
2009	1	280	0.000140	242.3	0.000165	252.3	0.000265	257.3
	2	313	0.000165	257.3	0.000190	267.3	0.000265	272.3
	3	342	0.000165	262.3	0.000190	272.3	0.000215	287.3
	4	10	0.000115	262.3	0.000115	287.3	0.000140	312.3
	5	38	0.000115	252.3	0.000065	267.3	0.000040	347.3
	6	69	0.000115	272.3	0.000065	282.3	0.000040	287.3
	7	100	0.000090	287.3	0.000040	277.3	0.000015	272.3
	8	131	0.000015	292.3	0.000015	342.3	0.000015	192.3
	9	160	0.000040	267.3	0.000040	227.3	0.000090	222.3
	10	187	0.000140	297.3	0.000115	247.3	0.000115	237.3
	11	216	0.000115	282.3	0.000140	272.3	0.000165	262.3
	12	247	0.000090	302.3	0.000115	287.3	0.000165	277.3

Table D1 (cont.): years 2010 to 2013

Year	Mon	L_S (deg)	C_R x A/m = 0.00 m^2/kg		C_R x A/m = 0.005m^2/kg		C_R x A/m = 0.01 m^2/kg	
			eccen	ω+Ω	eccen	ω+Ω	eccen	ω+Ω
2010	1	280	0.000040	332.3	0.000040	277.3	0.000115	282.3
	2	313	0.000065	282.3	0.000090	297.3	0.000165	297.3
	3	341	0.000040	302.3	0.000090	312.3	0.000140	307.3
	4	10	0.000065	332.3	0.000090	342.3	0.000140	347.3
	5	38	0.000090	352.3	0.000115	7.3	0.000165	7.3
	6	68	0.000090	22.3	0.000115	27.3	0.000140	37.3
	7	99	0.000065	27.3	0.000090	47.3	0.000115	57.3
	8	131	0.000015	337.3	0.000040	67.3	0.000065	77.3
	9	160	0.000065	342.3	0.000015	352.3	0.000015	322.3
	10	187	0.000090	7.3	0.000040	7.3	0.000015	7.3
	11	216	0.000140	37.3	0.000090	32.3	0.000040	32.3
	12	246	0.000140	47.3	0.000065	32.3	0.000040	17.3
2011	1	279	0.000140	27.3	0.000140	12.3	0.000140	357.3
	2	313	0.000215	42.3	0.000190	27.3	0.000215	17.3
	3	341	0.000215	47.3	0.000215	32.3	0.000265	27.3
	4	10	0.000165	57.3	0.000215	52.3	0.000240	42.3
	5	37	0.000115	57.3	0.000165	57.3	0.000215	52.3
	6	68	0.000115	42.3	0.000165	52.3	0.000215	57.3
	7	99	0.000190	37.3	0.000190	47.3	0.000215	57.3
	8	130	0.000265	47.3	0.000265	57.3	0.000265	62.3
	9	159	0.000265	62.3	0.000265	72.3	0.000290	77.3
	10	186	0.000215	62.3	0.000165	72.3	0.000140	92.3
	11	215	0.000265	57.3	0.000190	57.3	0.000165	62.3
	12	246	0.000265	62.3	0.000190	62.3	0.000140	62.3
2012	1	279	0.000240	72.3	0.000190	67.3	0.000140	57.3
	2	312	0.000190	67.3	0.000190	57.3	0.000165	42.3
	3	342	0.000190	67.3	0.000215	52.3	0.000215	42.3
	4	10	0.000240	62.3	0.000265	57.3	0.000340	52.3
	5	38	0.000315	67.3	0.000340	62.3	0.000415	62.3
	6	69	0.000315	77.3	0.000365	77.3	0.000415	72.3
	7	100	0.000240	72.3	0.000290	77.3	0.000390	82.3
	8	131	0.000315	72.3	0.000340	77.3	0.000365	82.3
	9	160	0.000340	82.3	0.000340	87.3	0.000340	92.3
	10	187	0.000290	87.3	0.000290	97.3	0.000265	107.3
	11	216	0.000215	87.3	0.000215	102.3	0.000190	112.3
	12	247	0.000215	82.3	0.000140	82.3	0.000090	87.3
2013	1	279	0.000290	77.3	0.000240	72.3	0.000190	62.3
	2	312	0.000340	82.3	0.000315	77.3	0.000290	72.3
	3	342	0.000340	87.3	0.000340	82.3	0.000315	77.3
	4	10	0.000315	97.3	0.000290	87.3	0.000315	77.3
	5	38	0.000290	92.3	0.000315	87.3	0.000365	82.3
	6	69	0.000315	97.3	0.000390	97.3	0.000415	92.3
	7	100	0.000290	107.3	0.000340	102.3	0.000390	102.3
	8	131	0.000240	112.3	0.000290	112.3	0.000340	117.3
	9	160	0.000215	107.3	0.000240	117.3	0.000290	122.3
	10	187	0.000265	97.3	0.000265	112.3	0.000290	122.3
	11	216	0.000340	102.3	0.000315	112.3	0.000265	122.3
	12	247	0.000340	112.3	0.000290	117.3	0.000265	127.3

Table D1 (cont.): years 2014 to 2017

Year	Mon	L_S (deg)	C_R x A/m = 0.00 m^2/kg eccen	$\omega+\Omega$	C_R x A/m = 0.005 m^2/kg eccen	$\omega+\Omega$	C_R x A/m = 0.01 m^2/kg eccen	$\omega+\Omega$
2014	1	280	0.000265	117.3	0.000215	127.3	0.000165	132.3
	2	313	0.000265	112.3	0.000215	112.3	0.000190	102.3
	3	341	0.000290	117.3	0.000265	107.3	0.000240	102.3
	4	10	0.000315	127.3	0.000290	122.3	0.000290	117.3
	5	38	0.000315	137.3	0.000290	132.3	0.000265	122.3
	6	68	0.000240	142.3	0.000240	137.3	0.000290	122.3
	7	99	0.000190	137.3	0.000265	127.3	0.000265	127.3
	8	131	0.000240	127.3	0.000315	127.3	0.000365	127.3
	9	160	0.000265	137.3	0.000315	137.3	0.000365	142.3
	10	187	0.000290	142.3	0.000340	152.3	0.000365	152.3
	11	216	0.000265	152.3	0.000290	157.3	0.000315	167.3
	12	246	0.000340	162.3	0.000265	162.3	0.000265	177.3
2015	1	279	0.000315	162.3	0.000290	172.3	0.000265	182.3
	2	313	0.000265	177.3	0.000240	182.3	0.000215	192.3
	3	341	0.000240	177.3	0.000215	177.3	0.000165	182.3
	4	10	0.000190	172.3	0.000165	162.3	0.000090	162.3
	5	37	0.000215	162.3	0.000190	152.3	0.000190	142.3
	6	68	0.000290	162.3	0.000315	152.3	0.000340	142.3
	7	99	0.000315	172.3	0.000315	162.3	0.000340	157.3
	8	130	0.000315	182.3	0.000340	177.3	0.000365	172.3
	9	159	0.000265	182.3	0.000290	182.3	0.000365	177.3
	10	186	0.000290	187.3	0.000340	187.3	0.000415	187.3
	11	215	0.000315	197.3	0.000365	202.3	0.000415	202.3
	12	246	0.000290	202.3	0.000340	212.3	0.000365	212.3
2016	1	279	0.000215	207.3	0.000240	217.3	0.000290	222.3
	2	312	0.000240	192.3	0.000215	207.3	0.000215	217.3
	3	342	0.000240	192.3	0.000215	202.3	0.000165	212.3
	4	10	0.000290	202.3	0.000240	202.3	0.000190	202.3
	5	38	0.000315	207.3	0.000265	207.3	0.000190	202.3
	6	69	0.000290	217.3	0.000240	207.3	0.000190	207.3
	7	100	0.000290	217.3	0.000290	202.3	0.000315	192.3
	8	131	0.000340	222.3	0.000365	212.3	0.000365	207.3
	9	160	0.000315	232.3	0.000340	222.3	0.000365	217.3
	10	187	0.000265	237.3	0.000290	232.3	0.000315	227.3
	11	216	0.000215	222.3	0.000265	222.3	0.000315	222.3
	12	247	0.000240	222.3	0.000290	222.3	0.000340	232.3
2017	1	279	0.000315	227.3	0.000340	232.3	0.000390	237.3
	2	312	0.000340	237.3	0.000365	242.3	0.000390	252.3
	3	342	0.000340	242.3	0.000340	247.3	0.000340	257.3
	4	10	0.000290	242.3	0.000265	252.3	0.000240	257.3
	5	38	0.000315	242.3	0.000240	247.3	0.000190	247.3
	6	69	0.000315	252.3	0.000265	252.3	0.000215	252.3
	7	100	0.000290	257.3	0.000240	257.3	0.000190	257.3
	8	131	0.000215	257.3	0.000190	247.3	0.000190	232.3
	9	160	0.000240	247.3	0.000240	237.3	0.000265	227.3
	10	187	0.000265	247.3	0.000315	242.3	0.000340	237.3
	11	216	0.000315	257.3	0.000365	257.3	0.000415	252.3
	12	247	0.000290	267.3	0.000365	262.3	0.000390	262.3

Table D1 (cont.): years 2018 to 2021

Year	Mon	L_S (deg)	C_R x A/m = 0.00 m^2/kg eccen	$\omega+\Omega$	C_R x A/m = 0.005 m^2/kg eccen	$\omega+\Omega$	C_R x A/m = 0.01 m^2/kg eccen	$\omega+\Omega$
2018	1	280	0.000240	262.3	0.000290	267.3	0.000365	272.3
	2	313	0.000315	262.3	0.000340	272.3	0.000365	277.3
	3	341	0.000315	272.3	0.000340	272.3	0.000340	287.3
	4	10	0.000290	282.3	0.000290	292.3	0.000315	297.3
	5	38	0.000215	287.3	0.000240	302.3	0.000240	312.3
	6	68	0.000165	287.3	0.000115	302.3	0.000090	312.3
	7	99	0.000190	267.3	0.000115	277.3	0.000065	257.3
	8	131	0.000240	277.3	0.000215	267.3	0.000165	267.3
	9	160	0.000265	287.3	0.000215	282.3	0.000215	272.3
	10	187	0.000240	297.3	0.000215	277.3	0.000215	272.3
	11	216	0.000215	292.3	0.000265	277.3	0.000265	272.3
	12	246	0.000240	302.3	0.000290	292.3	0.000315	282.3
2019	1	279	0.000190	312.3	0.000240	307.3	0.000290	302.3
	2	313	0.000140	327.3	0.000190	322.3	0.000240	322.3
	3	341	0.000140	327.3	0.000190	332.3	0.000265	337.3
	4	10	0.000115	312.3	0.000140	332.3	0.000190	337.3
	5	37	0.000140	307.3	0.000140	322.3	0.000140	342.3
	6	68	0.000190	312.3	0.000165	327.3	0.000190	342.3
	7	99	0.000215	332.3	0.000190	342.3	0.000165	352.3
	8	130	0.000165	347.3	0.000115	352.3	0.000140	12.3
	9	159	0.000140	327.3	0.000090	327.3	0.000065	307.3
	10	186	0.000165	342.3	0.000115	332.3	0.000090	322.3
	11	215	0.000165	2.3	0.000140	352.3	0.000115	342.3
	12	246	0.000165	12.3	0.000140	357.3	0.000115	342.3
2020	1	279	0.000115	17.3	0.000090	347.3	0.000115	332.3
	2	312	0.000090	352.3	0.000140	342.3	0.000190	337.3
	3	342	0.000115	352.3	0.000165	352.3	0.000215	347.3
	4	10	0.000165	7.3	0.000215	7.3	0.000265	7.3
	5	38	0.000165	22.3	0.000215	22.3	0.000290	27.3
	6	69	0.000165	32.3	0.000190	42.3	0.000265	47.3
	7	100	0.000165	32.3	0.000190	47.3	0.000215	57.3
	8	131	0.000240	37.3	0.000240	52.3	0.000240	57.3
	9	160	0.000215	52.3	0.000215	62.3	0.000215	72.3
	10	187	0.000165	62.3	0.000140	72.3	0.000140	87.3
	11	216	0.000115	52.3	0.000040	47.3	0.000015	52.3
	12	247	0.000115	37.3	0.000090	27.3	0.000090	12.3
2021	1	279	0.000215	47.3	0.000215	37.3	0.000190	22.3
	2	312	0.000265	62.3	0.000240	52.3	0.000190	42.3
	3	342	0.000265	67.3	0.000265	57.3	0.000265	52.3
	4	10	0.000215	72.3	0.000240	62.3	0.000265	47.3
	5	38	0.000215	67.3	0.000290	62.3	0.000365	57.3
	6	69	0.000265	72.3	0.000340	72.3	0.000390	72.3
	7	100	0.000265	77.3	0.000290	82.3	0.000365	82.3
	8	131	0.000215	77.3	0.000240	87.3	0.000265	92.3
	9	160	0.000190	72.3	0.000190	87.3	0.000215	97.3
	10	187	0.000240	72.3	0.000190	82.3	0.000190	92.3
	11	216	0.000290	77.3	0.000240	82.3	0.000215	87.3
	12	247	0.000290	87.3	0.000240	92.3	0.000165	92.3

Table D1 (cont.): years 2022 to 2025

Year	Mon	L_S (deg)	C_R x A/m = 0.00 m^2/kg eccen	$\omega+\Omega$	C_R x A/m = 0.005 m^2/kg eccen	$\omega+\Omega$	C_R x A/m = 0.01 m^2/kg eccen	$\omega+\Omega$
2022	1	280	0.000240	87.3	0.000190	82.3	0.000140	72.3
	2	313	0.000290	82.3	0.000290	72.3	0.000265	67.3
	3	341	0.000290	87.3	0.000290	77.3	0.000315	67.3
	4	10	0.000290	97.3	0.000290	92.3	0.000290	82.3
	5	38	0.000240	102.3	0.000265	92.3	0.000290	87.3
	6	68	0.000165	97.3	0.000215	92.3	0.000265	92.3
	7	99	0.000190	87.3	0.000215	92.3	0.000290	92.3
	8	131	0.000240	92.3	0.000290	97.3	0.000365	97.3
	9	160	0.000315	97.3	0.000340	102.3	0.000340	112.3
	10	187	0.000315	102.3	0.000290	117.3	0.000315	122.3
	11	216	0.000240	102.3	0.000215	107.3	0.000190	122.3
	12	246	0.000265	102.3	0.000240	107.3	0.000190	112.3
2023	1	279	0.000215	117.3	0.000165	117.3	0.000115	127.3
	2	313	0.000140	122.3	0.000090	117.3	0.000040	107.3
	3	341	0.000140	122.3	0.000090	117.3	0.000090	82.3
	4	10	0.000165	107.3	0.000165	97.3	0.000165	82.3
	5	37	0.000190	112.3	0.000240	102.3	0.000265	87.3
	6	68	0.000240	117.3	0.000290	107.3	0.000315	102.3
	7	99	0.000190	127.3	0.000240	122.3	0.000290	117.3
	8	130	0.000140	112.3	0.000190	117.3	0.000240	117.3
	9	159	0.000190	117.3	0.000190	127.3	0.000265	127.3
	10	186	0.000190	132.3	0.000215	142.3	0.000240	147.3
	11	215	0.000165	152.3	0.000190	167.3	0.000215	172.3
	12	246	0.000140	177.3	0.000140	177.3	0.000165	192.3
2024	1	279	0.000090	132.3	0.000065	177.3	0.000090	207.3
	2	312	0.000140	127.3	0.000090	127.3	0.000040	127.3
	3	342	0.000140	137.3	0.000090	132.3	0.000065	117.3
	4	10	0.000140	157.3	0.000090	147.3	0.000065	142.3
	5	38	0.000115	172.3	0.000090	152.3	0.000090	117.3
	6	69	0.000090	177.3	0.000115	142.3	0.000165	127.3
	7	100	0.000115	177.3	0.000140	162.3	0.000165	152.3
	8	131	0.000165	217.3	0.000190	182.3	0.000215	172.3
	9	160	0.000140	207.3	0.000165	197.3	0.000215	192.3
	10	187	0.000090	212.3	0.000140	202.3	0.000190	197.3
	11	216	0.000090	172.3	0.000115	197.3	0.000165	202.3
	12	247	0.000140	182.3	0.000140	197.3	0.000140	202.3
2025	1	279	0.000165	197.3	0.000165	217.3	0.000190	222.3
	2	312	0.000165	217.3	0.000190	232.3	0.000190	242.3
	3	342	0.000190	227.3	0.000190	242.3	0.000165	252.3
	4	10	0.000115	222.3	0.000040	172.3	0.000015	152.3
	5	38	0.000165	217.3	0.000090	212.3	0.000040	187.3
	6	69	0.000190	227.3	0.000140	217.3	0.000090	207.3
	7	100	0.000165	232.3	0.000140	222.3	0.000115	212.3
	8	131	0.000115	227.3	0.000115	207.3	0.000115	177.3
	9	160	0.000115	222.3	0.000140	207.3	0.000190	192.3
	10	187	0.000165	227.3	0.000215	222.3	0.000240	212.3
	11	216	0.000190	237.3	0.000240	232.3	0.000315	232.3
	12	247	0.000190	242.3	0.000265	247.3	0.000315	247.3

Table D2: Optimal Eccentricity Vector for C_R x A/m = 0.015, 0.02 & 0.03 m^2/kg

Year	Mon	L_S (deg)	C_R x A/m = 0.015 m^2/kg eccen	$\omega+\Omega$	C_R x A/m = 0.02 m^2/kg eccen	$\omega+\Omega$	C_R x A/m = 0.03 m^2/kg eccen	$\omega+\Omega$
2006	1	281	0.000065	187.3	0.000090	207.3	0.000115	237.3
	2	314	0.000015	247.3	0.000065	257.3	0.000140	272.3
	3	341	0.000090	77.3	0.000065	67.3	0.000040	357.3
	4	10	0.000065	107.3	0.000040	92.3	0.000140	32.3
	5	38	0.000090	127.3	0.000140	82.3	0.000215	67.3
	6	68	0.000140	107.3	0.000190	102.3	0.000265	87.3
	7	99	0.000190	117.3	0.000240	117.3	0.000365	107.3
	8	131	0.000240	137.3	0.000290	137.3	0.000390	137.3
	9	160	0.000265	157.3	0.000315	162.3	0.000415	162.3
	10	187	0.000240	177.3	0.000315	182.3	0.000415	182.3
	11	216	0.000240	207.3	0.000290	207.3	0.000415	212.3
	12	246	0.000215	232.3	0.000265	232.3	0.000365	237.3
2007	1	281	0.000190	232.3	0.000215	242.3	0.000290	257.3
	2	314	0.000165	247.3	0.000165	267.3	0.000290	272.3
	3	341	0.000115	257.3	0.000140	272.3	0.000140	312.3
	4	10	0.000015	287.3	0.000015	312.3	0.000090	7.3
	5	37	0.000040	112.3	0.000040	87.3	0.000115	67.3
	6	68	0.000115	142.3	0.000115	122.3	0.000190	102.3
	7	99	0.000165	172.3	0.000165	157.3	0.000215	132.3
	8	130	0.000165	187.3	0.000190	172.3	0.000265	162.3
	9	159	0.000190	197.3	0.000265	192.3	0.000365	177.3
	10	186	0.000290	207.3	0.000365	207.3	0.000440	202.3
	11	215	0.000340	227.3	0.000365	222.3	0.000465	222.3
	12	246	0.000365	242.3	0.000415	242.3	0.000515	247.3
2008	1	280	0.000265	257.3	0.000315	262.3	0.000440	267.3
	2	313	0.000165	277.3	0.000215	282.3	0.000340	287.3
	3	342	0.000115	287.3	0.000165	302.3	0.000265	312.3
	4	10	0.000040	312.3	0.000065	312.3	0.000140	352.3
	5	38	0.000040	262.3	0.000015	47.3	0.000090	37.3
	6	69	0.000015	172.3	0.000040	137.3	0.000090	102.3
	7	100	0.000140	187.3	0.000140	172.3	0.000190	152.3
	8	131	0.000215	212.3	0.000265	207.3	0.000265	182.3
	9	160	0.000190	222.3	0.000215	207.3	0.000290	197.3
	10	187	0.000215	227.3	0.000265	222.3	0.000340	212.3
	11	216	0.000240	237.3	0.000290	232.3	0.000415	232.3
	12	247	0.000240	247.3	0.000315	247.3	0.000415	247.3
2009	1	280	0.000315	262.3	0.000315	262.3	0.000440	267.3
	2	313	0.000315	277.3	0.000340	282.3	0.000440	287.3
	3	342	0.000265	292.3	0.000290	297.3	0.000365	307.3
	4	10	0.000165	317.3	0.000190	327.3	0.000290	337.3
	5	38	0.000090	357.3	0.000115	7.3	0.000215	12.3
	6	69	0.000040	42.3	0.000090	52.3	0.000190	62.3
	7	100	0.000015	102.3	0.000065	102.3	0.000190	97.3
	8	131	0.000065	172.3	0.000115	157.3	0.000190	137.3
	9	160	0.000115	207.3	0.000115	187.3	0.000240	187.3
	10	187	0.000165	227.3	0.000190	217.3	0.000290	212.3
	11	216	0.000215	252.3	0.000265	247.3	0.000340	242.3
	12	247	0.000215	272.3	0.000265	267.3	0.000390	262.3

Table D2 (cont.): years 2010 to 2013

Year	Mon	L_S (deg)	C_R x A/m = 0.015 m^2/kg		C_R x A/m = 0.02 m^2/kg		C_R x A/m = 0.03 m^2/kg	
			eccen	ω+Ω	eccen	ω+Ω	eccen	ω+Ω
2010	1	280	0.000165	282.3	0.000240	282.3	0.000340	282.3
	2	313	0.000215	297.3	0.000240	302.3	0.000340	307.3
	3	341	0.000165	332.3	0.000215	332.3	0.000340	332.3
	4	10	0.000190	357.3	0.000240	357.3	0.000340	7.3
	5	38	0.000190	17.3	0.000240	27.3	0.000340	32.3
	6	68	0.000190	42.3	0.000240	47.3	0.000365	52.3
	7	99	0.000190	67.3	0.000240	72.3	0.000290	82.3
	8	131	0.000090	92.3	0.000140	102.3	0.000215	112.3
	9	160	0.000040	142.3	0.000090	152.3	0.000190	147.3
	10	187	0.000015	192.3	0.000065	192.3	0.000190	192.3
	11	216	0.000015	262.3	0.000065	257.3	0.000165	242.3
	12	246	0.000090	312.3	0.000140	297.3	0.000215	282.3
2011	1	279	0.000165	347.3	0.000215	337.3	0.000265	322.3
	2	313	0.000240	12.3	0.000265	2.3	0.000340	352.3
	3	341	0.000290	22.3	0.000315	17.3	0.000390	7.3
	4	10	0.000265	32.3	0.000315	32.3	0.000415	27.3
	5	37	0.000265	47.3	0.000315	47.3	0.000440	47.3
	6	68	0.000240	57.3	0.000290	57.3	0.000415	62.3
	7	99	0.000290	62.3	0.000290	67.3	0.000415	77.3
	8	130	0.000315	72.3	0.000315	77.3	0.000415	87.3
	9	159	0.000290	87.3	0.000340	97.3	0.000340	107.3
	10	186	0.000165	97.3	0.000190	112.3	0.000240	132.3
	11	215	0.000065	62.3	0.000040	177.3	0.000090	177.3
	12	246	0.000090	57.3	0.000015	242.3	0.000015	247.3
2012	1	279	0.000090	42.3	0.000090	12.3	0.000140	317.3
	2	312	0.000165	22.3	0.000190	12.3	0.000265	357.3
	3	342	0.000240	32.3	0.000290	22.3	0.000390	17.3
	4	10	0.000390	47.3	0.000440	42.3	0.000515	37.3
	5	38	0.000440	57.3	0.000515	57.3	0.000615	57.3
	6	69	0.000465	72.3	0.000515	72.3	0.000640	72.3
	7	100	0.000415	82.3	0.000515	87.3	0.000590	87.3
	8	131	0.000365	87.3	0.000415	92.3	0.000515	97.3
	9	160	0.000365	102.3	0.000390	102.3	0.000465	117.3
	10	187	0.000290	112.3	0.000290	122.3	0.000340	137.3
	11	216	0.000165	127.3	0.000190	137.3	0.000215	162.3
	12	247	0.000040	87.3	0.000040	172.3	0.000090	192.3
2013	1	279	0.000165	57.3	0.000115	32.3	0.000015	247.3
	2	312	0.000240	62.3	0.000215	52.3	0.000215	42.3
	3	342	0.000340	67.3	0.000340	62.3	0.000365	47.3
	4	10	0.000365	72.3	0.000365	62.3	0.000465	52.3
	5	38	0.000440	77.3	0.000465	72.3	0.000565	67.3
	6	69	0.000490	87.3	0.000540	87.3	0.000640	87.3
	7	100	0.000465	102.3	0.000515	102.3	0.000615	102.3
	8	131	0.000390	117.3	0.000440	117.3	0.000540	122.3
	9	160	0.000315	127.3	0.000365	132.3	0.000465	137.3
	10	187	0.000315	127.3	0.000315	137.3	0.000390	147.3
	11	216	0.000290	127.3	0.000290	137.3	0.000290	162.3
	12	247	0.000240	132.3	0.000215	142.3	0.000165	177.3

Table D2 (cont.): years 2014 to 2017

Year	Mon	L_S (deg)	C_R x A/m = 0.015 m^2/kg		C_R x A/m = 0.02 m^2/kg		C_R x A/m = 0.03 m^2/kg	
			eccen	ω+Ω	eccen	ω+Ω	eccen	ω+Ω
2014	1	280	0.000140	142.3	0.000115	162.3	0.000090	187.3
	2	313	0.000140	97.3	0.000015	202.3	0.000015	237.3
	3	341	0.000215	92.3	0.000215	82.3	0.000215	62.3
	4	10	0.000290	107.3	0.000265	97.3	0.000315	82.3
	5	38	0.000290	112.3	0.000315	102.3	0.000365	92.3
	6	68	0.000290	117.3	0.000315	112.3	0.000415	102.3
	7	99	0.000365	117.3	0.000390	117.3	0.000515	117.3
	8	131	0.000415	127.3	0.000465	127.3	0.000565	127.3
	9	160	0.000415	142.3	0.000490	142.3	0.000590	147.3
	10	187	0.000415	157.3	0.000440	162.3	0.000540	167.3
	11	216	0.000365	172.3	0.000390	177.3	0.000515	187.3
	12	246	0.000315	182.3	0.000315	192.3	0.000415	207.3
2015	1	279	0.000240	192.3	0.000265	197.3	0.000265	217.3
	2	313	0.000190	202.3	0.000165	212.3	0.000165	227.3
	3	341	0.000140	197.3	0.000090	217.3	0.000040	272.3
	4	10	0.000090	132.3	0.000065	107.3	0.000115	72.3
	5	37	0.000215	127.3	0.000240	117.3	0.000265	97.3
	6	68	0.000340	137.3	0.000315	127.3	0.000390	117.3
	7	99	0.000390	152.3	0.000415	147.3	0.000465	137.3
	8	130	0.000390	167.3	0.000415	162.3	0.000465	157.3
	9	159	0.000390	177.3	0.000465	177.3	0.000565	172.3
	10	186	0.000465	187.3	0.000515	187.3	0.000615	187.3
	11	215	0.000440	207.3	0.000490	207.3	0.000640	207.3
	12	246	0.000415	217.3	0.000465	222.3	0.000565	227.3
2016	1	279	0.000315	232.3	0.000365	237.3	0.000440	242.3
	2	312	0.000215	232.3	0.000215	242.3	0.000290	262.3
	3	342	0.000140	222.3	0.000140	257.3	0.000165	282.3
	4	10	0.000140	202.3	0.000090	207.3	0.000015	332.3
	5	38	0.000140	202.3	0.000090	197.3	0.000040	87.3
	6	69	0.000190	182.3	0.000165	167.3	0.000240	142.3
	7	100	0.000315	187.3	0.000315	177.3	0.000340	162.3
	8	131	0.000365	202.3	0.000390	192.3	0.000440	182.3
	9	160	0.000365	217.3	0.000390	207.3	0.000465	197.3
	10	187	0.000365	217.3	0.000390	217.3	0.000490	212.3
	11	216	0.000365	222.3	0.000440	222.3	0.000540	222.3
	12	247	0.000390	232.3	0.000440	232.3	0.000540	237.3
2017	1	279	0.000415	242.3	0.000465	247.3	0.000565	252.3
	2	312	0.000415	257.3	0.000440	262.3	0.000540	267.3
	3	342	0.000365	267.3	0.000390	272.3	0.000440	282.3
	4	10	0.000240	277.3	0.000240	282.3	0.000265	302.3
	5	38	0.000140	252.3	0.000115	277.3	0.000115	322.3
	6	69	0.000165	252.3	0.000015	252.3	0.000015	37.3
	7	100	0.000140	237.3	0.000065	217.3	0.000065	157.3
	8	131	0.000190	207.3	0.000190	202.3	0.000215	182.3
	9	160	0.000290	222.3	0.000315	212.3	0.000390	202.3
	10	187	0.000365	232.3	0.000415	227.3	0.000515	222.3
	11	216	0.000465	247.3	0.000515	247.3	0.000615	242.3
	12	247	0.000440	262.3	0.000490	262.3	0.000640	257.3

Table D2 (cont.): years 2018 to 2021

Year	Mon	L_S (deg)	C_R x A/m = 0.015 m^2/kg		C_R x A/m = 0.02 m^2/kg		C_R x A/m = 0.03 m^2/kg	
			eccen	ω+Ω	eccen	ω+Ω	eccen	ω+Ω
2018	1	280	0.000415	272.3	0.000465	272.3	0.000565	272.3
	2	313	0.000415	277.3	0.000440	282.3	0.000565	287.3
	3	341	0.000365	287.3	0.000390	297.3	0.000465	302.3
	4	10	0.000315	307.3	0.000340	312.3	0.000390	327.3
	5	38	0.000215	317.3	0.000215	332.3	0.000265	347.3
	6	68	0.000090	332.3	0.000115	352.3	0.000140	22.3
	7	99	0.000015	247.3	0.000015	22.3	0.000065	62.3
	8	131	0.000140	262.3	0.000115	232.3	0.000015	122.3
	9	160	0.000190	257.3	0.000190	247.3	0.000215	217.3
	10	187	0.000215	262.3	0.000265	247.3	0.000340	227.3
	11	216	0.000315	267.3	0.000390	257.3	0.000465	252.3
	12	246	0.000365	282.3	0.000415	277.3	0.000515	272.3
2019	1	279	0.000340	302.3	0.000390	297.3	0.000515	297.3
	2	313	0.000290	317.3	0.000340	317.3	0.000465	317.3
	3	341	0.000315	337.3	0.000365	337.3	0.000465	337.3
	4	10	0.000215	347.3	0.000265	352.3	0.000390	357.3
	5	37	0.000190	357.3	0.000215	2.3	0.000315	17.3
	6	68	0.000165	352.3	0.000165	7.3	0.000215	32.3
	7	99	0.000140	7.3	0.000115	17.3	0.000140	47.3
	8	130	0.000140	27.3	0.000115	37.3	0.000115	67.3
	9	159	0.000040	302.3	0.000040	82.3	0.000065	117.3
	10	186	0.000065	307.3	0.000015	147.3	0.000040	162.3
	11	215	0.000090	317.3	0.000065	302.3	0.000140	252.3
	12	246	0.000090	317.3	0.000115	302.3	0.000215	277.3
2020	1	279	0.000165	307.3	0.000215	307.3	0.000315	302.3
	2	312	0.000265	337.3	0.000315	327.3	0.000415	322.3
	3	342	0.000265	347.3	0.000340	347.3	0.000440	347.3
	4	10	0.000315	12.3	0.000365	12.3	0.000490	12.3
	5	38	0.000365	32.3	0.000415	32.3	0.000490	32.3
	6	69	0.000315	52.3	0.000365	57.3	0.000490	57.3
	7	100	0.000290	62.3	0.000290	67.3	0.000390	77.3
	8	131	0.000215	72.3	0.000240	77.3	0.000340	92.3
	9	160	0.000215	82.3	0.000240	92.3	0.000265	107.3
	10	187	0.000115	107.3	0.000115	112.3	0.000140	137.3
	11	216	0.000015	117.3	0.000015	137.3	0.000040	177.3
	12	247	0.000090	357.3	0.000090	337.3	0.000115	302.3
2021	1	279	0.000165	12.3	0.000165	2.3	0.000190	332.3
	2	312	0.000215	27.3	0.000240	17.3	0.000290	357.3
	3	342	0.000290	42.3	0.000315	32.3	0.000415	22.3
	4	10	0.000315	47.3	0.000390	42.3	0.000465	37.3
	5	38	0.000390	57.3	0.000440	57.3	0.000540	52.3
	6	69	0.000440	72.3	0.000490	72.3	0.000615	72.3
	7	100	0.000390	87.3	0.000440	87.3	0.000565	87.3
	8	131	0.000315	102.3	0.000365	102.3	0.000465	107.3
	9	160	0.000240	107.3	0.000265	112.3	0.000340	127.3
	10	187	0.000165	112.3	0.000190	122.3	0.000240	142.3
	11	216	0.000190	97.3	0.000140	117.3	0.000115	157.3
	12	247	0.000140	102.3	0.000115	102.3	0.000015	272.3

Table D2 (cont.): years 2022 to 2025

Year	Mon	L_S (deg)	C_R x A/m = 0.015 m^2/kg eccen	$\omega+\Omega$	C_R x A/m = 0.02 m^2/kg eccen	$\omega+\Omega$	C_R x A/m = 0.03 m^2/kg eccen	$\omega+\Omega$
2022	1	280	0.000090	57.3	0.000090	27.3	0.000115	2.3
	2	313	0.000240	57.3	0.000240	47.3	0.000240	32.3
	3	341	0.000315	62.3	0.000340	52.3	0.000340	42.3
	4	10	0.000315	72.3	0.000340	67.3	0.000415	57.3
	5	38	0.000340	82.3	0.000365	77.3	0.000465	67.3
	6	68	0.000315	87.3	0.000365	87.3	0.000490	82.3
	7	99	0.000340	92.3	0.000415	92.3	0.000490	97.3
	8	131	0.000390	102.3	0.000465	102.3	0.000515	112.3
	9	160	0.000365	117.3	0.000440	117.3	0.000490	127.3
	10	187	0.000315	132.3	0.000365	137.3	0.000440	147.3
	11	216	0.000190	142.3	0.000215	162.3	0.000290	172.3
	12	246	0.000140	132.3	0.000090	157.3	0.000140	197.3
2023	1	279	0.000065	127.3	0.000015	232.3	0.000040	267.3
	2	313	0.000040	67.3	0.000040	32.3	0.000115	352.3
	3	341	0.000090	62.3	0.000090	42.3	0.000190	27.3
	4	10	0.000190	77.3	0.000240	67.3	0.000290	52.3
	5	37	0.000315	82.3	0.000390	77.3	0.000440	72.3
	6	68	0.000365	102.3	0.000415	97.3	0.000515	92.3
	7	99	0.000340	117.3	0.000390	112.3	0.000490	112.3
	8	130	0.000290	117.3	0.000365	117.3	0.000465	122.3
	9	159	0.000315	127.3	0.000365	137.3	0.000440	142.3
	10	186	0.000265	152.3	0.000315	162.3	0.000415	167.3
	11	215	0.000240	182.3	0.000265	182.3	0.000365	192.3
	12	246	0.000215	207.3	0.000240	212.3	0.000340	222.3
2024	1	279	0.000090	227.3	0.000140	237.3	0.000215	247.3
	2	312	0.000015	97.3	0.000040	287.3	0.000140	297.3
	3	342	0.000015	97.3	0.000015	317.3	0.000115	337.3
	4	10	0.000040	117.3	0.000090	52.3	0.000165	37.3
	5	38	0.000165	87.3	0.000190	82.3	0.000290	67.3
	6	69	0.000190	122.3	0.000265	112.3	0.000315	102.3
	7	100	0.000240	142.3	0.000290	137.3	0.000365	127.3
	8	131	0.000240	162.3	0.000290	162.3	0.000365	152.3
	9	160	0.000240	182.3	0.000290	182.3	0.000390	177.3
	10	187	0.000240	197.3	0.000290	197.3	0.000390	192.3
	11	216	0.000215	207.3	0.000240	207.3	0.000365	212.3
	12	247	0.000215	222.3	0.000240	222.3	0.000340	232.3
2025	1	279	0.000215	232.3	0.000240	237.3	0.000315	252.3
	2	312	0.000215	252.3	0.000240	257.3	0.000290	272.3
	3	342	0.000190	262.3	0.000165	277.3	0.000240	292.3
	4	10	0.000015	142.3	0.000065	317.3	0.000165	327.3
	5	38	0.000015	187.3	0.000015	352.3	0.000065	17.3
	6	69	0.000065	212.3	0.000065	102.3	0.000115	87.3
	7	100	0.000065	187.3	0.000090	147.3	0.000215	127.3
	8	131	0.000165	177.3	0.000215	167.3	0.000290	152.3
	9	160	0.000215	192.3	0.000265	182.3	0.000365	182.3
	10	187	0.000265	207.3	0.000340	207.3	0.000440	202.3
	11	216	0.000390	232.3	0.000390	227.3	0.000515	227.3
	12	247	0.000365	247.3	0.000440	247.3	0.000540	247.3

Table D3. Optimal Eccentricity Vector for C_R x A/m = 0.04, 0.05 & 0.06 m^2/kg

Year	Mon	L_S (deg)	C_R x A/m = 0.04 m^2/kg eccen	$\omega+\Omega$	C_R x A/m = 0.05 m^2/kg eccen	$\omega+\Omega$	C_R x A/m = 0.06 m^2/kg eccen	$\omega+\Omega$
2006	1	281	0.000215	252.3	0.000315	257.3	0.000415	267.3
	2	314	0.000190	297.3	0.000315	297.3	0.000415	302.3
	3	341	0.000165	352.3	0.000265	347.3	0.000390	347.3
	4	10	0.000215	22.3	0.000315	17.3	0.000440	17.3
	5	38	0.000315	57.3	0.000415	52.3	0.000540	52.3
	6	68	0.000390	87.3	0.000490	82.3	0.000615	82.3
	7	99	0.000465	107.3	0.000590	107.3	0.000665	107.3
	8	131	0.000515	132.3	0.000615	132.3	0.000715	132.3
	9	160	0.000515	162.3	0.000615	162.3	0.000715	157.3
	10	187	0.000490	187.3	0.000615	187.3	0.000715	187.3
	11	216	0.000515	212.3	0.000615	217.3	0.000715	217.3
	12	246	0.000515	242.3	0.000590	242.3	0.000715	242.3
2007	1	281	0.000390	262.3	0.000490	267.3	0.000615	267.3
	2	314	0.000365	282.3	0.000415	292.3	0.000515	297.3
	3	341	0.000265	322.3	0.000365	327.3	0.000465	332.3
	4	10	0.000190	7.3	0.000315	12.3	0.000415	12.3
	5	37	0.000215	57.3	0.000315	52.3	0.000415	47.3
	6	68	0.000290	92.3	0.000390	87.3	0.000515	82.3
	7	99	0.000315	117.3	0.000440	112.3	0.000515	112.3
	8	130	0.000390	142.3	0.000490	142.3	0.000565	142.3
	9	159	0.000465	177.3	0.000565	177.3	0.000640	172.3
	10	186	0.000540	197.3	0.000665	197.3	0.000790	197.3
	11	215	0.000590	222.3	0.000690	222.3	0.000815	222.3
	12	246	0.000615	247.3	0.000740	247.3	0.000865	247.3
2008	1	280	0.000540	267.3	0.000665	272.3	0.000765	272.3
	2	313	0.000440	292.3	0.000540	297.3	0.000640	297.3
	3	342	0.000365	317.3	0.000465	322.3	0.000565	327.3
	4	10	0.000240	357.3	0.000365	2.3	0.000490	7.3
	5	38	0.000215	42.3	0.000315	42.3	0.000440	42.3
	6	69	0.000140	92.3	0.000315	82.3	0.000390	82.3
	7	100	0.000240	132.3	0.000340	127.3	0.000440	117.3
	8	131	0.000315	167.3	0.000390	162.3	0.000465	152.3
	9	160	0.000365	187.3	0.000440	182.3	0.000540	172.3
	10	187	0.000440	207.3	0.000540	202.3	0.000665	202.3
	11	216	0.000490	227.3	0.000615	227.3	0.000740	227.3
	12	247	0.000540	247.3	0.000690	252.3	0.000790	252.3
2009	1	280	0.000565	272.3	0.000665	272.3	0.000790	272.3
	2	313	0.000515	292.3	0.000640	297.3	0.000740	297.3
	3	342	0.000465	312.3	0.000540	322.3	0.000640	322.3
	4	10	0.000390	347.3	0.000490	352.3	0.000590	357.3
	5	38	0.000290	22.3	0.000415	27.3	0.000540	32.3
	6	69	0.000315	62.3	0.000415	67.3	0.000515	67.3
	7	100	0.000290	97.3	0.000390	97.3	0.000515	97.3
	8	131	0.000290	137.3	0.000390	137.3	0.000490	137.3
	9	160	0.000315	177.3	0.000415	172.3	0.000515	172.3
	10	187	0.000390	207.3	0.000465	202.3	0.000590	202.3
	11	216	0.000415	237.3	0.000490	232.3	0.000615	232.3
	12	247	0.000515	262.3	0.000615	257.3	0.000715	257.3

Table D3 (cont.): years 2010 to 2013

Year	Mon	L_S (deg)	C_R x A/m = 0.04 m^2/kg eccen	$\omega+\Omega$	C_R x A/m = 0.05 m^2/kg eccen	$\omega+\Omega$	C_R x A/m = 0.06 m^2/kg eccen	$\omega+\Omega$
2010	1	280	0.000465	282.3	0.000565	282.3	0.000690	282.3
	2	313	0.000440	312.3	0.000565	307.3	0.000665	312.3
	3	341	0.000440	337.3	0.000540	337.3	0.000615	342.3
	4	10	0.000465	7.3	0.000565	7.3	0.000665	7.3
	5	38	0.000440	32.3	0.000565	32.3	0.000665	37.3
	6	68	0.000465	57.3	0.000590	62.3	0.000715	62.3
	7	99	0.000440	82.3	0.000515	87.3	0.000590	87.3
	8	131	0.000315	117.3	0.000440	117.3	0.000540	122.3
	9	160	0.000290	152.3	0.000390	152.3	0.000490	152.3
	10	187	0.000290	192.3	0.000390	192.3	0.000490	192.3
	11	216	0.000290	237.3	0.000390	232.3	0.000490	232.3
	12	246	0.000290	272.3	0.000440	267.3	0.000515	267.3
2011	1	279	0.000340	312.3	0.000490	302.3	0.000515	302.3
	2	313	0.000440	342.3	0.000515	337.3	0.000615	332.3
	3	341	0.000490	2.3	0.000615	2.3	0.000690	357.3
	4	10	0.000515	22.3	0.000615	22.3	0.000740	22.3
	5	37	0.000540	47.3	0.000665	47.3	0.000790	47.3
	6	68	0.000565	67.3	0.000665	67.3	0.000765	67.3
	7	99	0.000490	82.3	0.000565	87.3	0.000665	87.3
	8	130	0.000465	97.3	0.000540	102.3	0.000640	107.3
	9	159	0.000415	117.3	0.000490	122.3	0.000590	127.3
	10	186	0.000290	142.3	0.000365	152.3	0.000465	162.3
	11	215	0.000165	197.3	0.000265	202.3	0.000365	207.3
	12	246	0.000140	247.3	0.000265	247.3	0.000390	247.3
2012	1	279	0.000240	307.3	0.000340	297.3	0.000440	297.3
	2	312	0.000365	347.3	0.000465	337.3	0.000540	337.3
	3	342	0.000440	7.3	0.000565	7.3	0.000665	2.3
	4	10	0.000615	32.3	0.000715	32.3	0.000815	27.3
	5	38	0.000715	52.3	0.000840	52.3	0.000965	52.3
	6	69	0.000740	72.3	0.000865	72.3	0.000965	72.3
	7	100	0.000665	87.3	0.000815	92.3	0.000915	92.3
	8	131	0.000615	102.3	0.000715	107.3	0.000790	107.3
	9	160	0.000540	122.3	0.000590	132.3	0.000690	132.3
	10	187	0.000415	142.3	0.000490	152.3	0.000565	157.3
	11	216	0.000265	177.3	0.000340	187.3	0.000440	197.3
	12	247	0.000140	217.3	0.000215	222.3	0.000315	232.3
2013	1	279	0.000090	302.3	0.000165	302.3	0.000340	292.3
	2	312	0.000240	12.3	0.000315	347.3	0.000415	342.3
	3	342	0.000390	27.3	0.000465	17.3	0.000565	7.3
	4	10	0.000565	47.3	0.000640	37.3	0.000740	37.3
	5	38	0.000665	62.3	0.000815	62.3	0.000865	57.3
	6	69	0.000740	82.3	0.000840	82.3	0.000940	82.3
	7	100	0.000715	102.3	0.000815	102.3	0.000915	102.3
	8	131	0.000640	122.3	0.000765	122.3	0.000865	122.3
	9	160	0.000565	142.3	0.000665	142.3	0.000740	147.3
	10	187	0.000465	157.3	0.000565	162.3	0.000665	167.3
	11	216	0.000340	177.3	0.000415	187.3	0.000515	192.3
	12	247	0.000215	192.3	0.000265	212.3	0.000340	222.3

Table D3 (cont.): years 2014 to 2017

Year	Mon	L_S (deg)	C_R x A/m = 0.04 m^2/kg eccen	$\omega+\Omega$	C_R x A/m = 0.05 m^2/kg eccen	$\omega+\Omega$	C_R x A/m = 0.06 m^2/kg eccen	$\omega+\Omega$
2014	1	280	0.000090	222.3	0.000140	242.3	0.000240	257.3
	2	313	0.000015	287.3	0.000115	317.3	0.000215	317.3
	3	341	0.000240	42.3	0.000290	27.3	0.000365	22.3
	4	10	0.000340	67.3	0.000365	52.3	0.000465	47.3
	5	38	0.000440	82.3	0.000515	72.3	0.000615	67.3
	6	68	0.000515	97.3	0.000665	92.3	0.000740	87.3
	7	99	0.000615	112.3	0.000765	107.3	0.000865	107.3
	8	131	0.000665	127.3	0.000790	127.3	0.000890	127.3
	9	160	0.000690	147.3	0.000740	152.3	0.000865	152.3
	10	187	0.000640	172.3	0.000765	172.3	0.000890	172.3
	11	216	0.000590	192.3	0.000690	197.3	0.000815	202.3
	12	246	0.000490	217.3	0.000590	222.3	0.000690	227.3
2015	1	279	0.000315	237.3	0.000390	247.3	0.000515	257.3
	2	313	0.000190	272.3	0.000240	277.3	0.000340	287.3
	3	341	0.000065	327.3	0.000190	332.3	0.000290	337.3
	4	10	0.000190	52.3	0.000265	37.3	0.000365	32.3
	5	37	0.000340	82.3	0.000415	72.3	0.000515	67.3
	6	68	0.000490	112.3	0.000540	102.3	0.000640	97.3
	7	99	0.000540	132.3	0.000640	127.3	0.000740	122.3
	8	130	0.000590	152.3	0.000715	147.3	0.000790	147.3
	9	159	0.000640	172.3	0.000765	167.3	0.000865	167.3
	10	186	0.000740	187.3	0.000840	187.3	0.000940	187.3
	11	215	0.000715	212.3	0.000840	212.3	0.000965	212.3
	12	246	0.000690	227.3	0.000765	232.3	0.000890	232.3
2016	1	279	0.000540	252.3	0.000665	257.3	0.000740	257.3
	2	312	0.000390	272.3	0.000465	282.3	0.000565	287.3
	3	342	0.000215	302.3	0.000315	312.3	0.000440	317.3
	4	10	0.000090	7.3	0.000190	12.3	0.000315	12.3
	5	38	0.000115	72.3	0.000240	62.3	0.000340	62.3
	6	69	0.000265	127.3	0.000340	112.3	0.000415	102.3
	7	100	0.000415	152.3	0.000490	142.3	0.000540	137.3
	8	131	0.000515	177.3	0.000565	167.3	0.000665	162.3
	9	160	0.000540	192.3	0.000640	187.3	0.000740	182.3
	10	187	0.000615	207.3	0.000690	207.3	0.000790	207.3
	11	216	0.000640	222.3	0.000765	222.3	0.000865	222.3
	12	247	0.000665	242.3	0.000765	242.3	0.000890	242.3
2017	1	279	0.000665	257.3	0.000740	257.3	0.000865	262.3
	2	312	0.000615	277.3	0.000690	282.3	0.000765	287.3
	3	342	0.000490	292.3	0.000540	297.3	0.000615	307.3
	4	10	0.000340	317.3	0.000390	327.3	0.000490	337.3
	5	38	0.000190	352.3	0.000240	7.3	0.000340	17.3
	6	69	0.000090	62.3	0.000215	67.3	0.000340	67.3
	7	100	0.000165	127.3	0.000265	122.3	0.000415	117.3
	8	131	0.000315	167.3	0.000390	162.3	0.000465	152.3
	9	160	0.000440	192.3	0.000540	187.3	0.000665	187.3
	10	187	0.000615	217.3	0.000715	212.3	0.000815	207.3
	11	216	0.000715	237.3	0.000815	237.3	0.000915	237.3
	12	247	0.000740	257.3	0.000840	257.3	0.000940	257.3

Table D3 (cont.): years 2018 to 2021

Year	Mon	L_S (deg)	C_R x A/m = 0.04 m^2/kg eccen	$\omega+\Omega$	C_R x A/m = 0.05 m^2/kg eccen	$\omega+\Omega$	C_R x A/m = 0.06 m^2/kg eccen	$\omega+\Omega$
2018	1	280	0.000690	277.3	0.000815	277.3	0.000915	277.3
	2	313	0.000640	292.3	0.000740	292.3	0.000840	297.3
	3	341	0.000565	312.3	0.000640	317.3	0.000740	317.3
	4	10	0.000440	337.3	0.000515	342.3	0.000615	347.3
	5	38	0.000340	2.3	0.000415	12.3	0.000540	17.3
	6	68	0.000215	37.3	0.000315	47.3	0.000440	52.3
	7	99	0.000140	82.3	0.000240	82.3	0.000390	107.3
	8	131	0.000140	152.3	0.000240	147.3	0.000340	142.3
	9	160	0.000290	197.3	0.000365	187.3	0.000440	182.3
	10	187	0.000415	222.3	0.000515	217.3	0.000615	212.3
	11	216	0.000565	247.3	0.000640	242.3	0.000740	242.3
	12	246	0.000615	272.3	0.000740	267.3	0.000840	267.3
2019	1	279	0.000615	292.3	0.000715	292.3	0.000840	292.3
	2	313	0.000565	317.3	0.000690	317.3	0.000815	317.3
	3	341	0.000565	337.3	0.000665	337.3	0.000765	337.3
	4	10	0.000490	2.3	0.000590	2.3	0.000690	2.3
	5	37	0.000440	22.3	0.000540	27.3	0.000640	32.3
	6	68	0.000315	42.3	0.000415	52.3	0.000515	57.3
	7	99	0.000240	62.3	0.000340	77.3	0.000440	82.3
	8	130	0.000165	97.3	0.000240	102.3	0.000340	117.3
	9	159	0.000115	137.3	0.000190	142.3	0.000315	152.3
	10	186	0.000115	182.3	0.000240	192.3	0.000365	192.3
	11	215	0.000265	237.3	0.000340	232.3	0.000540	237.3
	12	246	0.000315	272.3	0.000440	262.3	0.000615	267.3
2020	1	279	0.000415	297.3	0.000540	292.3	0.000640	292.3
	2	312	0.000515	322.3	0.000615	322.3	0.000715	317.3
	3	342	0.000565	347.3	0.000665	347.3	0.000790	347.3
	4	10	0.000590	12.3	0.000690	12.3	0.000815	12.3
	5	38	0.000640	37.3	0.000740	37.3	0.000840	37.3
	6	69	0.000590	62.3	0.000715	62.3	0.000865	62.3
	7	100	0.000515	82.3	0.000665	82.3	0.000715	87.3
	8	131	0.000415	102.3	0.000515	107.3	0.000590	112.3
	9	160	0.000315	117.3	0.000390	132.3	0.000465	142.3
	10	187	0.000215	152.3	0.000290	167.3	0.000540	177.3
	11	216	0.000140	212.3	0.000240	217.3	0.000415	217.3
	12	247	0.000190	272.3	0.000265	272.3	0.000490	257.3
2021	1	279	0.000240	312.3	0.000340	302.3	0.000465	297.3
	2	312	0.000365	337.3	0.000465	337.3	0.000540	332.3
	3	342	0.000465	12.3	0.000565	7.3	0.000640	2.3
	4	10	0.000565	32.3	0.000690	32.3	0.000790	27.3
	5	38	0.000665	52.3	0.000765	52.3	0.000890	47.3
	6	69	0.000715	72.3	0.000840	72.3	0.000890	72.3
	7	100	0.000665	92.3	0.000765	92.3	0.000890	92.3
	8	131	0.000565	112.3	0.000640	117.3	0.000765	117.3
	9	160	0.000440	132.3	0.000540	137.3	0.000640	142.3
	10	187	0.000315	157.3	0.000390	162.3	0.000490	167.3
	11	216	0.000165	182.3	0.000265	197.3	0.000390	197.3
	12	247	0.000065	242.3	0.000190	247.3	0.000290	247.3

Table D3 (cont.): years 2022 to 2025

Year	Mon	L_S (deg)	C_R x A/m = 0.04 m^2/kg eccen	$\omega+\Omega$	C_R x A/m = 0.05 m^2/kg eccen	$\omega+\Omega$	C_R x A/m = 0.06 m^2/kg eccen	$\omega+\Omega$
2022	1	280	0.000165	342.3	0.000215	312.3	0.000340	297.3
	2	313	0.000265	12.3	0.000315	357.3	0.000390	342.3
	3	341	0.000390	27.3	0.000515	22.3	0.000540	12.3
	4	10	0.000515	47.3	0.000590	42.3	0.000690	37.3
	5	38	0.000565	62.3	0.000665	62.3	0.000765	57.3
	6	68	0.000590	82.3	0.000740	77.3	0.000840	77.3
	7	99	0.000615	97.3	0.000715	97.3	0.000840	97.3
	8	131	0.000640	112.3	0.000740	112.3	0.000815	117.3
	9	160	0.000590	132.3	0.000715	132.3	0.000765	142.3
	10	187	0.000490	152.3	0.000590	157.3	0.000690	162.3
	11	216	0.000365	182.3	0.000490	192.3	0.000590	197.3
	12	246	0.000240	217.3	0.000365	227.3	0.000465	232.3
2023	1	279	0.000165	272.3	0.000290	272.3	0.000390	277.3
	2	313	0.000190	332.3	0.000290	327.3	0.000390	322.3
	3	341	0.000265	7.3	0.000390	2.3	0.000490	2.3
	4	10	0.000415	42.3	0.000515	37.3	0.000565	32.3
	5	37	0.000540	67.3	0.000640	62.3	0.000740	57.3
	6	68	0.000615	87.3	0.000715	87.3	0.000815	87.3
	7	99	0.000590	107.3	0.000715	107.3	0.000865	102.3
	8	130	0.000590	122.3	0.000690	122.3	0.000890	127.3
	9	159	0.000540	147.3	0.000640	147.3	0.000740	147.3
	10	186	0.000490	172.3	0.000615	177.3	0.000690	177.3
	11	215	0.000490	202.3	0.000590	207.3	0.000690	207.3
	12	246	0.000440	227.3	0.000515	232.3	0.000590	232.3
2024	1	279	0.000340	257.3	0.000440	262.3	0.000540	267.3
	2	312	0.000240	307.3	0.000340	307.3	0.000465	302.3
	3	342	0.000215	347.3	0.000315	347.3	0.000440	347.3
	4	10	0.000290	32.3	0.000390	27.3	0.000490	22.3
	5	38	0.000390	62.3	0.000465	57.3	0.000565	57.3
	6	69	0.000440	92.3	0.000515	87.3	0.000665	87.3
	7	100	0.000440	122.3	0.000565	117.3	0.000690	112.3
	8	131	0.000465	152.3	0.000565	147.3	0.000665	142.3
	9	160	0.000465	172.3	0.000590	172.3	0.000665	167.3
	10	187	0.000490	192.3	0.000615	192.3	0.000715	192.3
	11	216	0.000490	217.3	0.000615	217.3	0.000715	217.3
	12	247	0.000440	237.3	0.000540	242.3	0.000640	242.3
2025	1	279	0.000415	257.3	0.000540	262.3	0.000615	267.3
	2	312	0.000390	282.3	0.000490	287.3	0.000590	292.3
	3	342	0.000290	307.3	0.000390	312.3	0.000465	322.3
	4	10	0.000240	342.3	0.000315	347.3	0.000415	357.3
	5	38	0.000165	32.3	0.000265	37.3	0.000365	37.3
	6	69	0.000215	77.3	0.000315	77.3	0.000440	77.3
	7	100	0.000290	117.3	0.000465	112.3	0.000515	112.3
	8	131	0.000390	147.3	0.000490	147.3	0.000590	147.3
	9	160	0.000465	177.3	0.000565	177.3	0.000665	172.3
	10	187	0.000540	202.3	0.000615	202.3	0.000740	197.3
	11	216	0.000640	227.3	0.000765	227.3	0.000890	227.3
	12	247	0.000640	247.3	0.000740	247.3	0.000840	247.3

SMC Standard Improvement Proposal

INSTRUCTIONS

1. Complete blocks 1 through 7. All blocks must be completed.
2. Send to the Preparing Activity specified in block 8.

NOTE: Do not use this form to request copies of documents, or to request waivers, or clarification of requirements on current contracts. Comments submitted on this form do not constitute or imply authorization to waive any portion of the referenced document(s) or to amend contractual requirements. Comments submitted on this form do not constitute a commitment by the Preparing Activity to implement the suggestion; the Preparing Authority will coordinate a review of the comment and provide disposition to the comment submitter specified in Block 6.

SMC STANDARD CHANGE RECOMMENDATION:	**1. Document Number**	**2. Document Date**
3. Document Title		

4. Nature of Change
(Identify paragraph number; include proposed revision language and supporting data. Attach extra sheets as needed.)

5. Reason for Recommendation

6. Submitter Information

a. Name	**b. Organization**
c. Address	**d. Telephone**
e. E-mail address	**7. Date Submitted**

8. Preparing Activity

Space and Missile Systems Center
AIR FORCE SPACE COMMAND
483 N. Aviation Blvd.
El Segundo, CA 91245
Attention: SMC/EAE

March 2008